Monetary Policy and the Long-Run Trend of Treasury Yields

Zehao Li*

October 2023

Abstract

Secular declines in U.S. Treasury yields almost entirely happened within three-day event windows around FOMC announcement dates. Cumulative yield changes during these short windows can explain the secular decline in the yield curve. This factor contains essential information on excess bond returns orthogonal to observed yields and outperforms well-known proxies for interest rate trends in predicting excess bond returns. Attributing the trend to the cumulative effects of monetary policy, we estimate a dynamic term structure model with an unspanned stochastic trend to explain these empirical facts. The model can be applied to daily data and is thus amenable to high-frequency studies of monetary policy transmission. We propose a regression-based estimation algorithm that can be executed instantaneously. The model suggests that the secular declines in Treasury yields over the past three decades were primarily due to reductions in expected interest rates. Monetary policy mainly reduced expected interest rates before the ZLB episode and compressed term premia between late 2008 and early 2012 on FOMC announcement dates.

Keywords: Monetary policy, yield curve, secular decline in yields.
JEL Codes: E43, E52

*The Chinese University of Hong Kong, Shenzhen. 2001 Longxiang Blvd, Shenzhen, Guangdong, China 518172. E-mail: lizehao@cuhk.edu.cn. We thank Di Wu, Yilin David Yang, Zhengyang Xu, and seminar participants at the City University of Hong Kong for their helpful comments.

1 Introduction

Expected interest rates are a crucial channel through which monetary policy affects the economy. The U.S. policy rate has decreased steadily over the past three decades, so it is reasonable that expected interest rates should reflect this downward trend. However, standard new Keynesian and affine term structure models suggest that expected interest rates must revert to a constant at long maturities because the models assume that the short-term interest rate is stationary. We build a dynamic term structure model to reconcile the empirical fact with model implications. The model shows that the cumulative effects of monetary policy have caused secular declines in all Treasury yields by reducing the long-run expectations of interest rates and contains crucial information about excess bond returns beyond observed yields.

U.S. Treasury yields have been shifting downwards since the 1980s. The literature has found that persistent variations in macroeconomic variables are essential for determining the downward trend of interest rates. For example, trend inflation, the real interest rate trend, and the nominal short-term interest rate trend all contain important information about the fluctuations in the long-run expectations of interest rates, that is, their stochastic trends. Meanwhile, monetary policy strongly influences the yield curve. The short end is closely tied to the policy interest rate, and the medium- to long-term yields are also related through no-arbitrage conditions. An important open question is whether the secular decline in the yield curve is attributable to monetary policy and what components of the yield curve are mainly responsible for the fall.

We quantify the critical effects of monetary policy on the secular trends in U.S. Treasury yields in two steps. First, we establish some empirical facts about monetary policy and Treasury yield trends. One crucial point is that the cumulative changes in Treasury yields during three-day windows around monetary policy announcement dates contain essential information for predicting excess bond returns. The prediction performance is superior to existing proxies for the persistent variations in interest rates such as trend inflation (π_t^*), natural interest rate (r_t^*), and trend nominal interest rate ($i_t^* \equiv \pi_t^* + r_t^*$). Second, we estimate a dynamic term structure model with shifting endpoints to account for the trend explicitly. According to this model, significant fractions of expected yields decline during FOMC announcement dates, while monetary policy has much smaller effects on risk premia.

A simple illustration of the critical effects of monetary policy on the secular decline in yields is provided in Figure 1. The construction of the series follows Hillenbrand (2021). For each yield, the red curve assumes that it changes only during the three-day event windows from the day before to the day after the FOMC announcement dates (FOMC windows). In other words, we set the daily yield changes outside the event windows to zero and cumulatively sum the daily changes over time. We label the changes in the n-year yield during the FOMC windows $\nabla y_t^{(n)}$ and denote the first principal component across all maturities by ∇y_t. The grey curve depicts the cumulative yield changes outside the three-day event windows. Since 1990, the changes in yields during FOMC windows have steadily decreased and fitted the observed yield series closely. In contrast, the cumulative changes outside the FOMC windows appear stationary.

Figure 1 about here.

This strong link between yield changes during FOMC windows and Treasury yield trends is the core of our analysis. We establish two stylized facts about FOMC windows and Treasury yield trends. First, the first principal component[1] of the changes in all yields during FOMC windows captures the common downward trend for Treasury yields. We show this in a cointegration regression and a VAR model with unobserved trends (Del Negro et al. (2017b), Harvey (1989)). In the VAR exercise, we allow for common and yield-specific trends for each yield. The former is highly correlated with ∇y_t while the latter is almost flat. It corroborates the well-known fact that the nominal Treasury yields of different maturities are cointegrated (Campbell and Shiller (1987), Hall et al. (1992)), and we establish that the cointegration trend is caused by monetary policy. There is a long tradition of relating the interest rate trend to the declining trend of inflation, such as Kozicki and Tinsley (2001) and Cieslak and Povala (2015), but Bauer and Rudebusch (2020) document that trend inflation "leaves a highly persistent component of interest rates unexplained" and that the trend real interest rate is also necessary for explaining Treasury yield trends. Similar to Bauer and Rudebusch (2020), we attribute the common trend for Treasury yields to a nominal interest rate trend. A crucial difference is that our trend variable, ∇y_t, is explicitly related to monetary policy, whereas the trend variable in Bauer and Rudebusch (2020) is attributed to the natural interest rate and trend inflation. Our interest rate trends over the last three decades were determined on a few special dates. In contrast, existing explanations of interest rate trends, including Bauer and Rudebusch (2020), suggest that the trends behaved smoothly and no sets of dates were significantly more consequential than others for determining the trends.

Our second stylized fact is that the yield changes during the FOMC windows are crucial for explaining bond risk premia. Treasury yields are cointegrated with ∇y_t. Deviations of yields from ∇y_t quickly revert, with 50% of the deviation eliminated within a quarter. Consequently, ∇y_t helps predict future yields and excess bond returns. For the same reason, the

[1]Like the observed yields, the first principal component of the cumulative changes during FOMC windows can be interpreted as the average level across all maturities. See Figure 3 for an illustration.

literature has found that including proxies for the cointegration trend in predictive regressions for excess bond returns results in substantial gains in predictive power. For example, Cieslak and Povala (2015) add the long-run inflation trend π_t^* and Bauer and Rudebusch (2020) include long-run nominal interest rate i_t^* in the predictive regressions and find statistically and economically significant coefficients on the trend variables and considerable improvements in the R^2. Cieslak and Povala (2015) argue that trend inflation controls the expected yields component in observed yields that is orthogonal to the risk premium. We find similar results for ∇y_t, but we also find that ∇y_t contains essential information about the term premium component that is orthogonal to observed yields. Overall, ∇y_t better captures the cointegration trend of Treasury yields and further improves the predictive power relative to existing proxies for interest rate trends.

We estimate a dynamic term structure model with a stochastic trend in the state vector to understand how monetary policy shapes the yield curve. We incorporate ∇y_t as the empirical proxy for the stochastic trend of states. A crucial difference from canonical dynamic term structure models is that those models assume that the state variables follow a stationary VAR process. By construction, those models imply that expected short-term yields in the long-run future converge to a constant, and thus, fluctuations in the long-term yields must be captured by risk premia. On the contrary, our model allows stochastic variations in the limiting long-term expectations of short-term yields. Thus, the secular declines in the long-term yields can be due to falling expected short-term yields.

Using the dynamic term structure model, we find that the expected short-term yields (risk-neutral yields) have decreased substantially since 1990 and that a significant fraction occurred during the three-day FOMC windows. For example, the 10-year risk-neutral yield has declined by 7.5 percentage points since 1990 and by 5.2 percentage points during the FOMC windows. Meanwhile, the term premia decreased by 2.5 percentage points during the FOMC windows. We also regress changes in risk-neutral yields and term premia during FOMC windows on high-frequency monetary policy shocks. The responses of risk-neutral yields are several times stronger than the responses of term premia. For example, the 10-year risk-neutral yield increases by 0.56 percentage points when the policy rate unexpectedly increases by one percentage point, while the 10-year term premium only increases by 0.08 percentage points. The analysis implies that the effects of monetary policy on Treasury yields are mainly attributable to responses of risk-neutral yields, which is consistent with the predictions of standard new Keynesian models.

In the dynamic term structure model, we define interest rate trends as the "endpoints", which are the long-run limits of expected yields[2]: $y_t^{(n)*} = \lim_{s\to\infty} \mathbf{E}_t \left[y_{t+s}^{(n)} \right]$, where $y_{t+s}^{(n)}$ is

[2]Note that the endpoints differ from risk-neutral yields. The risk-neutral yield for maturity n is the

the n-year yield at time $t+s$. Our model shows that $y_t^{(n)*}$ for all maturities can be well approximated by linear transformations of ∇y_t, which is consistent with the cointegration regression results. The model implies that a reduction in the policy rate announced by the FOMC leads to a permanent downward shift in the long-run expectations of the entire yield curve. Therefore, expected future short-term yields and risk-neutral yields decrease. This point is, again, consistent with the monetary policy transmission mechanism in standard new Keynesian models that monetary policy mainly affects expected interest rates. However, standard new Keynesian models are stationary, and thus $y_t^{(n)*}$ is constant by construction. To this end, our analysis suggests that monetary policy shocks can have larger and more persistent effects than implied by standard new Keynesian monetary models.

Our empirical identification strategy is related to the monetary policy literature using high-frequency shocks. The key assumption is that the only factor affecting interest rates during the short event window around the FOMC announcement is the monetary policy decision. We follow this strategy to identify ∇y_t as a consequence of monetary policy decisions, similar to, for example, Gürkaynak et al. (2005a) and Hanson and Stein (2015). A common practice in this literature is to regress dependent variables on high-frequency monetary policy shocks to study the *marginal effects* of monetary policy. We contribute to the literature by documenting that the *cumulative effects* of monetary policy accounts for most of the variations in the yield curve.

A modeling contribution of our paper is that our model can be estimated at high frequencies, and the estimation is fast because we rely on a regression approach that avoids numerical optimizations. Our empirical proxy for the trend is available at the daily or even intraday frequency. Macroeconomic trend variables are usually observed at low frequencies, monthly at best. For example, the dynamic term structure model with shifting endpoints in Bauer and Rudebusch (2020) is estimated at the quarterly frequency because the key variable, the trend interest rate, is observed quarterly. This is problematic when we analyze the effects of monetary policy shocks on the yield curve using high-frequency regressions, such as Hanson and Stein (2015). Since our proxy for the trend comes from daily yield changes on specific event dates, it is easy to construct and amenable to analyzing term premia at high frequencies.

Related Literature A large body of literature studies the effects of monetary policy on the yield curve. The standard approach is to regress changes in yields or forward rates,

average expected short-term yields between t and $t+n$. For example, the 10-year risk-neutral yield is $\frac{1}{n}\mathbf{E}_t\left[\sum_{s=0}^{9} y_{t+s}^{(1)}\right] + constant$, while the endpoint for the 10-year yield is $y_t^{(10)*} = \lim_{s\to\infty}\mathbf{E}_t\left[y_{t+s}^{(10)}\right]$. In stationary affine term structure models, the former can vary over time, but the latter is constant.

usually within short event windows containing monetary policy announcements, on estimated monetary policy shocks or study the impulse responses of yields to the monetary policy shock in a structural VAR. For example, Kuttner (2001), Gürkaynak et al. (2005a,b), Hanson and Stein (2015), and Bauer and Swanson (2022b) show that high-frequency monetary policy shocks have significant effects on short- to long-term yields. Using VAR methods, Wright (2012), Gertler and Karadi (2015), and Jarociński and Karadi (2020) also find consistent results. Our analysis studies the cumulative effects of monetary policy. A closely related paper is Hillenbrand (2021), which documents that the secular declines in U.S. Treasury yields since the late 1980s almost entirely occurred during the three-day FOMC windows. We extend his analysis to show that the cumulative effects of monetary policy contain important information on expected future short yields and the term premia and help explain interest rate trends in a structural model.

The secular decline in interest rates has drawn wide attention. Popular explanations of the secular decline include the global savings glut (Bernanke (2005)), a lack of capital investment opportunities (Summers (2014)), a slowdown in productivity growth (Gordon (2017)), a fall in the price of capital (Eichengreen (2015)), demographic changes (Gagnon et al. (2021), Carvalho et al. (2016)), and an increase in the liquidity of Treasury securities (Del Negro et al. (2017a)). Hillenbrand (2021) documents that the secular decline happens within short event windows around FOMC announcements, and we explore the implications of the FOMC trend for predicting interest rates.

A benchmark for predicting excess bond returns uses linear combinations of current yields as predictors, such as Fama and Bliss (1987), Campbell and Shiller (1991), and Cochrane and Piazzesi (2005) among many others. It is widely documented that current yields don't contain all the information about future yields and incorporating macroeconomic predictors significantly improves predictive power (Kozicki and Tinsley (2001), Ludvigson and Ng (2009), Duffee (2013), Joslin et al. (2014), Cieslak and Povala (2015), Bauer and Rudebusch (2017), Bauer and Hamilton (2018), Bauer and Rudebusch (2020)). Our contribution is to document that the cumulative effects of monetary policy serve as a critical macroeconomic trend and capture essential information about the risk-neutral yield and term premia components of the yield curve.

Canonical dynamic term structure models assume that the state variables determining the yields follow a stationary VAR process (e.g., Kim and Wright (2005), Wright (2011), Joslin et al. (2011), Gürkaynak and Wright (2012), Adrian et al. (2013)). These models are ill-suited for studying the determinants of interest rate trends because long-run expected short-term rates converge to the unconditional mean. Incorporating a random walk trend in the state vector, Bauer and Rudebusch (2020) find that the secular declines in interest rates are mostly due to reductions in long-run expected yields driven by the downward trend in the nominal short rate. We also find that the expectations hypothesis component drives the majority of the secular decline, but we relate the time-varying long-run expectation to the cumulative effects of monetary policy. Piazzesi (2005) includes monetary policy rate as an observed state variable in an affine term structure model and finds that monetary policy helps match the whole yield curve. A key difference is that Piazzesi (2005) uses the federal funds target rate to measure monetary policy, while we use the cumulative sum of high-frequency interest rate shocks. We show that the latter fits the yield trends better. Furthermore, the monetary policy variable is spanned by the yields in Piazzesi (2005), but not in our term structure model. The latter is consistent with our regression results that adding the monetary policy variable significantly improves the predictive power for excess bond returns relative to observed yields.

The rest of the paper is organized as follows. Section 2 formally describes the construction of ∇y_t and presents evidence that long-run trends in monetary policy and Treasury yields are cointegrated. Section 3 estimates excess bond return prediction regressions to show that the yield changes during FOMC windows contain important information about the yield curve that the observed yields don't capture. Section 4 estimates a dynamic term structure model with a stochastic trend to explain the empirical facts and study the effects of monetary policy on risk-neutral yields and term premia. Section 5 examines whether the monetary policy trend simply reflects its reactions to macroeconomic trends and shows that monetary policy has unique roles for determining interest rate trends. Section 6 concludes.

2 FOMC and the Yield Curve

2.1 The FOMC Filter

We apply the Hillenbrand (2021) filter to daily U.S. Treasury yields estimated by the Federal Reserve Board using the method of Gürkaynak et al. (2007). The filter divides the sample into two parts: FOMC windows consisting of dates $t-1, t, t+1$ for each FOMC announcement date t, and non-FOMC windows consisting of the rest dates. Then, the filter computes the cumulative sums of daily yield changes on each subsample. Equivalently, the filter assumes that the yields only change within a given subsample and remain constant on the other. Following Hillenbrand (2021), our sample starts from June 5, 1989.

Formally, the filter is defined as

$$\nabla y_t^{(n),W} = y_{t_0}^{(n)} + \sum_{s=t_0+1}^{t} \left(y_s^{(n)} - y_{s-1}^{(n)} \right) \mathbf{1}_W \left(s \right), \tag{1}$$

where t and s denote daily dates, t_0 is the first date of the sample, $y_s^{(n)}$ is the log n-year Treasury zero coupon yield on date s, $\mathbf{1}_W()$ is an indicator function for the set W, and $W \in \{FOMC, non-FOMC\}$ is the set of dates either for the FOMC or the non-FOMC window. In the following, we denote the FOMC-window changes in the n-year yield by $\nabla y_t^{(n)}$ and the first principal component of the FOMC-window changes in all yields by ∇y_t, unless we need to distinguish the FOMC-window from the non-FOMC-window series.

As shown in Figure 1, changes during the FOMC windows almost perfectly capture the secular declines in different yields. Figure 2 collects cumulative yield changes during FOMC announcement windows for different maturities in the top panel and plots the observed yields of the respective maturities in the bottom panel. Overall, short-term yields have declined more than medium- to long-term yields during FOMC windows, but there is clearly a common downward trend for all series. The dispersion across different maturities in the top panel is more stable than in the bottom panel, indicating a more stable slope of the FOMC-filtered yield curve than the observed one. The stable slope of the cumulative yield changes during the FOMC windows suggests that monetary policy affects different yields in roughly constant proportions, indicating that the short-rate expectations component should be more affected by monetary policy than the term premia. We show more formal evidence of this point in Section 3 and Section 4.

Interestingly, rises and falls in the federal funds rate do not appear to have symmetric effects on Treasury yields, especially for medium and long maturities. The federal funds rate increased steadily around 1995, between 2005 and 2008, between 2015 and 2019, and from 2022 to now. But these increases in the policy rate were not accompanied by increases in the medium- and long-term Treasury yields, except for the most recent period. This is also true for changes during the FOMC window. When the FOMC increased the federal funds rate during monetary policy meetings, the Treasury yields barely increased. Even for the most recent tightening episode, Treasury yields did not increase much during FOMC windows. The discrepancy in behaviors between the federal funds rate and Treasury yields suggests that changes in Treasury yields during the FOMC windows are more informative about the yield curve dynamics than changes in the federal funds rate. This is why we do not use the federal funds target rate as a state variable for the yield curve as in Piazzesi (2005), and we show that the federal funds target rate is not a good proxy for interest rate trends in

Section 4.

Figure 2 about here.

The similarity between the two panels in Figure 2 motivates a representation of the FOMC-window series by the principal components as the case for observed yields. In Figure 3, we summarize the yield curve and its filtered components by their first three principal components. The weighting matrix is normalized such that each principal component's weights on all yields sum to 1. The cumulative changes in yields during FOMC windows inherit a similar factor structure as the original yields: the first principal component accounts for 97% of the total variation, and the second accounts for almost the remaining variation; the factor loadings prompt the level, slope, and curvature interpretations of the first three principal components. The level factors of the observed and the FOMC-window yields are highly correlated, and the latter accounts for almost all the downward trends of the former. The slope factor of observed yields is more volatile than that of the FOMC-filtered yields.

Figure 3 about here.

2.2 Yield Changes and Monetary Policy Shocks

Observed changes in the Treasury yields during the FOMC windows are caused by monetary policy, but monetary policy endogenously responds to macroeconomic conditions. How much do the daily changes in the Treasury yields around FOMC announcement dates reflect the causal effects of monetary policy? To distill the unexpected interest rate changes caused by monetary policy, a standard approach in the monetary policy literature uses changes in the Fed Funds futures rates or Eurodollar futures rates around FOMC press releases to measure unexpected changes in monetary policy (for example, Kuttner (2001); Gürkaynak et al. (2005b,a); Bauer and Swanson (2022a,b). Some other authors use observed changes in Treasury yields during the same FOMC windows as ours to measure monetary policy changes (e.g., Hanson and Stein (2015)).

We compare the cumulative sums of high-frequency Eurodollar futures shocks[3] with the cumulative changes in Treasury yields during the three-day FOMC announcement windows. The Eurodollar shocks are changes in the futures rates on ED1-ED4, the contracts that expire in the current quarter up to three quarters in the future, during 30-minute windows

[3] The data are obtained from Michael Bauer's webpage for replication materials for Bauer and Swanson (2022b). We plot the Eurodollar futures shocks because the sample coverage is longer. Gürkaynak et al. (2007) show that Eurodollar futures are the best predictors of future federal funds rates at horizons beyond 6 months and are as good as Fed Funds futures at horizons less than 6 months.

around FOMC announcements. For the Treasury yields, we focus on the 1- and 10-year yields to represent the short and long ends of the yield curve.

Table 1 presents summary statistics of the Eurodollar futures shocks and the FOMC-window changes in the 1- and 10-year yields. All variables are summed within each month. The mean values are negative but within one standard deviation away from zero. Compared with the 3-day changes in the observed yields, the Eurodollar shocks are closer to zero on average and less volatile. However, the extreme values of the Eurodollar shocks and the changes in observed yields have similar magnitudes. For example, the minimum values of the ED1 shocks and the 10-year yield changes are -0.55 and -0.45 percentage points, and the maximum values of the ED4 shocks and 1-year yield changes are 0.24 and 0.26 percentage points, respectively.

Table 1 about here.

Although the literature uses the high-frequency interest rate futures shocks as proxies for mean-zero monetary policy shocks and the mean values of the Eurodollar futures shocks are indeed indistinguishable from zero, their cumulative sums over time exhibit clear downward trends. Figure 4 plots cumulative sums of the intraday Eurodollar futures rates on FOMC announcement dates, as well as the daily changes in the 1- and 10-year Treasury yields from the day before to the day after FOMC announcement dates[4]. We plot the end-of-month values of each series. The cumulative changes in the intraday Eurodollar futures rates and Treasury yields all exhibit strong downward trends in the sample, which are highly correlated. The cumulative sums of high-frequency Eurodollar futures shocks declined by 4 percentage points over the last three decades, and $\nabla y_t^{(10)}$ declined by 6 percentage points. The figure suggests that the daily changes in the Treasury yields around FOMC press release dates are good proxies for the causal effects of monetary policy.

In summary, the cumulative changes in Treasury yields during three-day FOMC announcement windows strongly correlate with the cumulative sums of monetary policy shocks. Therefore, we use the cumulative changes in Treasury yields to summarize the historical stances of monetary policy.

Figure 4 about here

2.3 Unit Roots and Cointegration

It is well-known that nominal Treasury yields are persistent and can be modeled as unit-root processes. We investigate whether the cumulative effects of monetary policy an-

[4]Between meetings, the series remain at the values observed at the previous announcement window. In this way, we obtain daily values for these series.

nouncements can account for the trend in Treasury yields using cointegration regressions and error correction models. Formally, we estimate a dynamic OLS regression for cointegrated processes $(y_t^{(n)}, \boldsymbol{\tau}_t)$:

$$y_t^{(n)} = \beta_0 + \boldsymbol{\beta}_1^\top \boldsymbol{\tau}_t + u_t, \tag{2}$$

where $y_t^{(n)}$ is a Treasury yield, $\boldsymbol{\tau}_t$ is a scalar or vector of proxies for the trend. Following Stock and Watson (1993), we include leads and lags of the first-differenced $y_t^{(n)}$ and $\boldsymbol{\tau}_t$ in the regression to estimate β_0 and $\boldsymbol{\beta}_1$. We focus on the 10-year yield and choose four leads and lags. The trend proxies include the trend inflation π_t^*, trend real interest rate r_t^*, trend nominal interest rate i_t^*, and the first principal component of cumulative changes in all yields during FOMC windows ∇y_t. In Appendix C, we report estimation results for the first principal component of all yields, which can be interpreted as the average across all maturities. Due to the availability of the macroeconomic trend series, the data are quarterly and range from 1989Q2 to 2018Q1.

Table 2 reports the point estimates $\hat{\beta}_0$ and $\hat{\boldsymbol{\beta}}_1$ as well as persistence test statistics for the cointegration residuals $\hat{u}_t = y_t^{(n)} - \hat{\beta}_0 - \hat{\boldsymbol{\beta}}_1^\top \boldsymbol{\tau}_t$. The standard errors for the regression coefficients are Newey-West with six lags. The first column regresses $y_t^{(10)}$ on a constant, so the residual is the demeaned yield. The first-order autocorrelation coefficient ($\hat{\rho}$) is 0.95 and the Augmented Dickey-Fuller (ADF) and Phillips-Perron (P.P.) unit root tests do not reject the null hypothesis that the demeaned yield has a unit root. Moreover, the low-frequency stationary test of Müller and Watson (2013) strongly rejects stationarity. These results are consistent with the well-known fact that interest rates are highly persistent.

The second column of Table 2 regresses cumulative changes in the 10-year yield outside FOMC windows ($\nabla y_t^{(10),non-FOMC}$) on a constant and tests whether the residual contains a unit root. The intercept term is 8.48 percentage points, while the initial value of the 10-year yield in our sample is 8.56 percentage points. This indicates that, on average, the 10-year yield barely changed between FOMC meetings during the last three decades. In contrast, the average value of the 10-year yield on the full sample is 4.78, indicating a significant secular decline. The first-order autocorrelation coefficient of $\nabla y_t^{(10),non-FOMC}$ is much smaller than that of $y_t^{(10)}$, and all test statistics strongly indicate that $\nabla y_t^{(10),non-FOMC}$ is stationary. Note that the FOMC and non-FOMC windows are disjoint, and any date belongs to one of them,

$$1 = \mathbf{1}_{FOMC}(s) + \mathbf{1}_{non-FOMC}(s), \quad \forall s. \tag{3}$$

So, the filtered yields on the two sets of dates must sum up to the observed yield:

$$y_t^{(n)} - y_0^{(n)} = \left(\nabla y_t^{(n),FOMC} - y_0^{(n)}\right) + \left(\nabla y_t^{(n),non-FOMC} - y_0^{(n)}\right). \tag{4}$$

The first two columns of Table 2 suggest that the 10-year yield contains a persistent stochastic trend, but the second term on the right-hand side does not, so the unit root of the 10-year yield must be due to the cumulative effects of monetary policy announcements $\nabla y_t^{(10),FOMC}$.

The remaining columns of Table 2 report the results of cointegration regressions using different trend proxies as independent variables. We consider macroeconomic trends, including trend inflation (π_t^*), trend inflation and natural interest rate (r_t^*), and trend nominal interest rate ($i_t^* = \pi_t^* + r_t^*$). These macroeconomic trends are compared with ∇y_t to study whether the roles of monetary policy in determining the yield curve merely reflect the impacts of macroeconomic activities. The first specification includes only π_t^*, which is motivated by Cieslak and Povala (2015). The resulting cointegration residual is almost as persistent as the 10-year yield, and the test statistics find no evidence for stationarity. The inadequacy of detrending with only π_t^* suggests that the role of monetary policy in detrending the yields should not be interpreted as a Taylor rule that responds only to changes in inflation. Using a combination of π_t^* and r_t^*, or i_t^*, or ∇y_t as the detrending variable, the cointegration residuals are much less persistent than the original 10-year yield. Among these residuals, the one produced by ∇y_t has the most significant statistics against the unit root hypothesis and the weakest statistic against stationarity. Furthermore, the error-correction coefficient is estimated as -0.46 and is strongly significant. When the 10-year yield is high relative to ∇y_t, it quickly reverts to this trend, with half of the difference eliminated within a quarter. Therefore, knowing the cumulative effect of monetary policy is quite helpful in predicting Treasury yields.

Although the residuals produced by i_t^* and ∇y_t exhibit similar persistence properties, the regression coefficients on the two variables are quite different. The trend nominal interest rate i_t^* has a coefficient of 2.03 in the cointegration regression, while ∇y_t has a coefficient of 1.27. Accordingly, the yield moves almost one-to-one with the long-run trend of monetary policy, and hence, simply subtracting the latter from the former produces a stationary residual. The large slope coefficient suggests that the trend nominal interest rate is "flatter" than the trend of the Treasury yield. If trend variables are used without scaling up or down to proxy the trend of the Treasury yield, the long-run trend of monetary policy provides the best fit.

In summary, the persistent variations in Treasury yields are well explained by the cumulative effects of monetary policy, which appear to be quite different from simply reacting to macroeconomic conditions. In Table A1, we report the results for detrending the first principal component of all yields. Interestingly, the only residuals for which the ADF and P.P. tests significantly reject the unit root hypothesis are the demeaned $\nabla y_t^{non-FOMC}$ and the regression residual produced by ∇y_t.

Table 2 about here.

2.4 A Trend-VAR Model

Motivated by the results of the cointegration regressions, we estimate a VAR model with unobservable trends to further illustrate that monetary policy can explain a common trend for all yields. The VAR model also sets the stage for the state structure of our dynamic term structure model in Section 4.

We estimate an $N \times 1$ vector process Y_t that can be decomposed as

$$Y_t = \Gamma \bar{Y}_t + \tilde{Y}_t, \tag{5}$$

where $\bar{Y}_t$ is an $\bar{N} \times 1$ vector of stochastic trends, Γ is an $N \times \bar{N}$ matrix of loadings on the trends, and $\tilde{Y}_t$ is an $N \times 1$ vector of stationary component. The vector $Y_t = (Y_t^{(n)\top}, \nabla y_t)^\top$ consists of a set of Treasury yields, $Y_t^{(n)}$, and the first principal component of the FOMC window yields, ∇y_t. The dynamics for the trend and stationary components are, respectively:

$$\begin{aligned} \bar{Y}_t =& \bar{Y}_{t-1} + \eta_t, \\ \tilde{Y}_t =& \Phi(L)\tilde{Y}_{t-1} + \tilde{u}_t, \end{aligned} \tag{6}$$

where $\Phi(L) = \sum_{l=1}^{p} \Phi_l L^l$ is a polynomial of lag operators with all eigenvalues within the unit circle. The $(\bar{N} + N) \times 1$ vector of shocks is i.i.d and distributed as

$$\begin{bmatrix} \eta_t \\ \tilde{u}_t \end{bmatrix} \sim \mathcal{N}\left(\begin{bmatrix} 0_{\bar{N}} \\ 0_N \end{bmatrix}, \begin{bmatrix} \Omega_\eta & 0_{\bar{N}\times N} \\ 0_{N\times\bar{N}} & \Omega_{\tilde{u}} \end{bmatrix} \right). \tag{7}$$

The initial conditions $\bar{y}_0$ and $\tilde{y}_{0:-p+1} \equiv (\tilde{y}_0^\top, \ldots, \tilde{y}_{-p+1}^\top)^\top$ are distributed as

$$\begin{aligned} \bar{y}_0 \sim& \mathcal{N}\left(\underline{y_0}, \underline{V_0}\right), \\ \tilde{y}_{0:-p+1} \sim& \mathcal{N}\left(0, V(\Phi, \Omega_{\tilde{u}})\right), \end{aligned} \tag{8}$$

where $V(\Phi, \Omega_{\tilde{u}})$ is the unconditional variance of $\tilde{y}_{0:-p+1}$ implied by Equation (6).

The model is estimated using the Bayesian method in Del Negro et al. (2019). The priors for the VAR coefficients and covariance matrices have a standard form:

$$\begin{aligned} p(\boldsymbol{\varphi}|\Omega_{\tilde{u}}) =& \mathcal{N}(\text{vec}(\underline{\boldsymbol{\Phi}}), \Omega_{\tilde{u}} \otimes \underline{\Omega})\mathcal{I}(\boldsymbol{\varphi}), \\ p(\Omega_\eta) =& \mathcal{IW}(\kappa_\eta, (\kappa_\eta + N + 1)\underline{\Omega_\eta}), \\ p(\Omega_{\tilde{u}}) =& \mathcal{IW}(\kappa_{\tilde{u}}, (\kappa_{\tilde{u}} + \bar{N} + 1)\underline{\Omega_{\tilde{u}}}), \end{aligned} \tag{9}$$

where $\boldsymbol{\Phi} = (\Phi_1, \ldots, \Phi_p)^\top$ is the collection of VAR coefficients and $\boldsymbol{\varphi} \equiv \text{vec}(\boldsymbol{\Phi})$, $\mathcal{I}.\mathcal{W}.(\kappa, (\kappa +$

$m+1)\underline{\Omega}$) denotes the inverse Wishart distribution with mode $\underline{\Omega}$ and κ degrees of freedom, and $\mathcal{I}(\boldsymbol{\varphi})$ is an indicator function that equals 0 if the VAR is explosive and 1 otherwise. The prior for Γ is Gaussian with a diagonal covariance matrix.

The prior for Ω_η is conservative to limit the amount of variation attributed to trends. The matrix $\underline{\Omega_\eta}$ is diagonal with elements $6^2/1200$, which implies that the standard deviation of the expected change in the trend nominal interest rate over one century is 6 percentage points. We set $\kappa_\eta = 100$ so that the priors are tight. The priors for the VAR parameters describing $\tilde{Y}$ are standard Minnesota priors, with the hyperparameter for the overall tightness equal to the commonly used value of 0.2, except that the prior for the own-lag parameter is centered at 0 instead of 1. The prior for the variance $\Omega_{\tilde{u}}$ is an inverse Wishart distribution centered at a diagonal matrix of 1s, with $N+2$ degrees of freedom.

We include the 3-month, 5-year, and 10-year Treasury yields in the vector $Y_t^{(n)} = (y_t^{(0.25)}, y_t^{(5)}, y_t^{(10)})^\top$. The trend vector includes yield-specific trends and a common trend: $\bar{Y}_t = (\bar{Y}_t^{(n)\top}, \bar{y}_t)^\top$, where $\bar{Y}_t^{(n)}$ is an $(N-1)\times 1$ vector of yield-specific trends, and $\bar{N} = N$. The loading matrix is

$$\Gamma = \begin{bmatrix} \boldsymbol{I}_{N-1} & \Gamma^{(n)}_{(N-1)\times 1} \\ \mathbf{0}_{1\times(N-1)} & 1, \end{bmatrix} \tag{10}$$

so that the trend for each yield is $\Gamma^{(n)}\bar{y}_t + \bar{y}_t^{(n)}$ and the trend for ∇y_t is $\bar{y}_t$. Under this specification, we allow the yield-specific trend $\bar{y}_t$ to capture the persistent variations in $y_t^{(n)}$ that are not captured by the cointegration relationship. Our sample consists of end-of-month observations from January 1990 to December 2022.

In the previous literature, the focus on inflation and real interest rate (Del Negro et al. (2017b), Cieslak and Povala (2015), Bauer and Rudebusch (2020)) is motivated by the Fisher equation $i_t = r_t + \pi_t$. Analogously, our formulation can also be viewed as another decomposition of observed yields. Equation (4) implies that any time series can be decomposed as the sum of cumulative changes during the FOMC windows and outside the FOMC windows. So, the specification $\gamma^{(n)}\bar{y}_t + \bar{y}_t^{(n)}$ can be viewed as decomposing the trend of $y_t^{(n)}$ into trends of cumulative changes during and outside the FOMC windows, respectively.

Figure 5 presents the estimates of the common trend and yield-specific trends. The common trend $\bar{y}_t$ almost coincides with ∇y_t with a narrow 95% confidence band, indicating that ∇y_t accounts for a common trend for the Treasury yield curve. For each yield, the common trend component, $\gamma^{(n)}\bar{y}_t$, is almost parallel to the yield's overall trend, and the yield-specific trend, $\bar{y}_t^{(n)}$, is essentially flat. Therefore, ∇y_t contributes to the time variations in the long-run trends of Treasury yields, and the yield-specific trends act mainly as level shifters. This is consistent with the cointegration regression results in Table 2: the observed Treasury yields are cointegrated with average changes in yields during FOMC announcement windows, and the cointegration residuals are stationary.

Figure 5 about here.

Figure 5 and Table 2 suggest that the persistent variations in Treasury yields can be summarized by a single component closely related to ∇y_t. Therefore, we model the yield curve as containing a single stochastic trend in Section 4 and use ∇y_t as the empirical proxy for the stochastic trend.

3 Predicting Excess Bond Returns

When the yields are cointegrated, the trend serves as an anchor for interest rate dynamics. Therefore, the literature has found that proxies for the trend help predict excess bond returns. For example, Cieslak and Povala (2015) find that trend inflation captures the expectations hypothesis component embedded in yields and helps predict excess bond returns. Bauer and Rudebusch (2020) show that the downward-trending long-run nominal interest, i_t^*, helps predict future excess returns on long-term bonds. Motivated by these facts and the fact that the yield changes within the FOMC windows account for substantial fractions of the persistent variations in interest rates, we investigate whether ∇y_t also helps predict excess bond returns and performs better than existing proxies for the trend of interest rates.

3.1 Baseline Regression

We estimate the equation

$$\overline{rx}_{t+1} = \alpha + \boldsymbol{PC}_t^\top \boldsymbol{\beta} + \gamma \tau_t + \varepsilon_{t+1}, \tag{11}$$

where $\overline{rx}_{t+1} = \frac{1}{14}\sum_{n=2}^{15} rx_{t+1}^{(n)}$ is the average excess bond return, $rx_{t+1}^{(n)} = -(n-1)y_{t+1}^{(n-1)} + ny_t^{(n)} - y_t^{(1)}$ is the one-year[5] excess return on the n-year bond, $\boldsymbol{PC}_t$ is the first three principal components of the $1, 2, \ldots, 15$-year yields, and τ_t is a trend variable. Our candidates for τ_t include estimates of the inflation trend π_t^*, the real-rate trend r_t^*, the long-run nominal short rate $i_t^* = \pi_t^* + r_t^*$, and the first principal component of FOMC-window yields ∇y_t.

The estimates of π_t^* and r_t^* are borrowed from Bauer and Rudebusch (2020), who, in turn, combine their own estimates of r_t^* with other authors' estimates (Del Negro et al. (2017b); Johannsen and Mertens (2016); Laubach and Williams (2016); Holston et al. (2017); Kiley

[5]We report results for the quarterly holding period in Appendix C. Although the R^2s are uniformly smaller than in the annual case, ∇y_t still significantly improves predictive power.

(2020)). For detailed descriptions of the estimates of r_t^* and π_t^*, please refer to Bauer and Rudebusch (2020).

Table 3 shows the regression results. Besides Newey-West standard errors in parentheses, we also present small-sample bootstrap p-values à la Bauer and Hamilton (2018) in square brackets. Columns (1) through (6) run the same regressions as in Bauer and Rudebusch (2020) (Table 2) but on different samples. In the full sample (1989-2018) and the 1994-2018 subsample, both i_t^* and ∇y_t significantly increase the predictive coefficient on the level factor (PC1) and the R^2 relative to the model with only the yield curve principal components. Furthermore, ∇y_t has a better predictive performance than i_t^*. The coefficient on ∇y_t is highly significant with a smaller p-value than i_t^*, and the regression with ∇y_t has an R^2 9 percentage points higher than the R^2 with i_t^*. The improvement in R^2 is the same in both samples, although the post-1994 sample produces uniformly higher R^2s than the full sample. The coefficient on ∇y_t is negative, implying that when currently observed yields are higher than the cumulative effects of monetary policy (or, ∇y_t decreases), future yields are expected to decrease, and bond prices will increase, so the holding period return is expected to increase. This is consistent with the results of the cointegration regressions in Table 2.

Table 3 about here.

3.2 Investigating the Mechanisms

To further investigate the predictive mechanism of ∇y_t, we conduct three sets of regressions. First, we investigate whether ∇y_t alone captures time variations in the expected yields or term premia. Then, we study why including ∇y_t in Equation (11) significantly improves the prediction performance, and we conduct two regressions. First, we study whether the yield curve component orthogonal to ∇y_t significantly predicts excess bond returns. Second, we study whether the ∇y_t component orthogonal to the observed yields significantly predicts excess bond returns.

We start by estimating the regression

$$\overline{rx}_{t+1} = \alpha + \gamma \tau_t + \varepsilon_{t+1}, \tag{12}$$

which is equivalent to restricting $\boldsymbol{\beta} = \mathbf{0}$ in Equation (11). If the expectations hypothesis holds, $rx_{t+1}^{(n)}$ consists of solely innovations to the conditional expectations of future short-term yields, which are orthogonal to time-t information. Therefore, significant regressors in the excess bond return regressions are interpreted as capturing the time-varying term premia. In Table 4, the trending variables are all insignificant, and the R^2s are close to zero. Therefore, the trend variables alone don't capture the variations in the term premia, but control the expectations hypothesis component in $\boldsymbol{PC}_t$ in Equation (11). This finding echoes the result of Cieslak and Povala (2015, eq. (28)). Note that ∇y_t has a positive coefficient, indicating that when Treasury yields decrease (not holding other factors constant) during the FOMC window, term premia also decrease. This is consistent with Figure 8, which shows that term premia have declined during FOMC windows since 1990.

Table 4 about here.

Next, we investigate why ∇y_t significantly improves the prediction performance relative to observed yields. By the Frisch-Waugh-Lovell theorem, the regression coefficient on $\boldsymbol{PC}_t$ in Equation (11) equals the one from regressing $\overline{rx}_{t+1}$ on the orthogonalized $\boldsymbol{PC}_t$, and the latter is the residual from regressing $\boldsymbol{PC}_t$ on τ_t. The coefficient on τ_t is obtained similarly. Motivated by this observation, we investigate whether the orthogonalized yields or the orthogonalized trend contains information about excess bond returns.

First, we estimate

$$\overline{rx}_{t+1} = \alpha + \widetilde{\boldsymbol{PC}}_t^\top \boldsymbol{\beta} + \varepsilon_{t+1}, \tag{13}$$

where $\widetilde{\boldsymbol{PC}}_t^\top$ denotes the first three principal components of the residuals from regressions of each yield on the trend variables. Note that we first orthogonalize the yields and then take the principal components. So, $\widetilde{\boldsymbol{PC}}_t$ is not the orthogonalized $\boldsymbol{PC}_t$ in the Frisch-Waugh-Lovell theorem. Table 5 presents the results. Here, we want $\widetilde{\boldsymbol{PC}}_t$ to summarize all the information in the orthogonalized yields instead of only orthogonalized three principal components. Column (1) uses $\boldsymbol{PC}_t$ as independent variables. Columns (2) to (6) use $\widetilde{\boldsymbol{PC}}_t$ obtained from regressing on respective trend variables. Finally, column (7) uses the first three principal components of changes in yields outside the FOMC windows, that is, applying Equation (1) to non-FOMC windows. This is motivated by the identity Equation (4), although the decomposition does not guarantee orthogonality between the two components on the right side.

In Table 5, the largest R^2s are obtained in column (6), where the yields are orthogonalized relative to ∇y_t. According to the results in Table 4, ∇y_t controls the expectations hypothesis component of the observed yields, so the remaining part of the yields orthogonal to the expectations hypothesis component better predicts excess bond returns. The coefficient in PC1 improves from 0.58 to 2.25, suggesting that the cyclical fluctuations of the yield curve levels relative to the trends induced by monetary policy strongly correlate with the term premia. In columns (6) and (7), the level factors (PC1) have similar coefficients significantly higher than that on the level of observed yields. Non-FOMC yield changes also achieve a similar R^2 with the yield components orthogonal to ∇y_t, implying that monetary policy mainly affects expected yields, and non-monetary policy factors drive the term premia. Columns (6) and (7) jointly imply that deviations of yields from the monetary policy trend revert quickly and thus are strongly informative about future yields.

Table 5 about here.

Next, we estimate

$$\overline{rx}_{t+1} = \alpha + \gamma\tilde{\tau}_t + \varepsilon_{t+1}, \tag{14}$$

where $\tilde{\tau}_t$ is the residual from regressing the trend τ_t on all observed yields. Table 6 presents the results. Orthogonalized trend inflation is insignificant and achieves an almost zero R^2. As noted by Cieslak and Povala (2015), the trend inflation captures the expectations hypothesis component that is orthogonal to the variation in the risk premium. Combining or summing with r_t^* increases the coefficient on π_t^* and R^2. The trend real interest rate contains information on both expected yields and risk premia that is orthogonal to the observed yields. This is consistent with the view of Bauer and Rudebusch (2020):"*Accounting only for the inflation trend on its own, ..., leaves a highly persistent component of interest rates unexplained.*" In our regression results, orthogonalized ∇y_t has a coefficient similar to orthogonalized i_t^*, but the R^2 obtained by the former more than doubles the R^2 obtained by the latter. This is strong evidence that ∇y_t contains significantly more information on the term premia than i_t^* that is orthogonal to the observed yields.

Table 6 about here.

Since the short-term nominal interest rate is persistent, it is straightforward that monetary policy affects expected future short rates. The literature also finds that monetary policy shocks move the term premia. For example, Hanson and Stein (2015) find evidence that monetary policy shocks affect long-term forward rates' expectations and risk premium components. Consistent with the literature, our excess bond return regressions provide new evidence that monetary policy shapes the expected future short yields and risk premia. Moreover, the two components in ∇y_t offset each other, so the coefficient on ∇y_t is insignificant in Equation (12).

4 A Term Structure Model with a Stochastic Trend

In this section, we estimate a no-arbitrage dynamic term structure model. The model highlights the following points:

1. The cumulative effects of monetary policy, ∇y_t, determine the persistent variations in interest rates.

2. ∇y_t helps predict excess bond returns.

3. The secular declines in interest rates were mainly due to reductions in risk-neutral yields, which occurred mostly when FOMC announced monetary policy decisions.

The dynamic term structure model is proposed by Bauer and Rudebusch (2020). Importantly, we attribute the trend to a different macroeconomic variable and estimate the model using linear regressions, significantly improving the estimation speed.

We use lowercase letters to represent scalars and uppercase or bold letters to denote vectors and matrices. The state vector X_t consists of K linear combinations of yields. As a standard practice in yield curve modeling, we choose the first five principal components of the 3-month, 6-month, and 1- to 15-year yields as X_t. Section 2 showed that the yields are cointegrated, so we model the vector X_t as driven by a scalar stochastic trend τ_t:

$$X_t = \boldsymbol{\mu} + \Gamma\tau_t + \tilde{X}_t, \quad \tau_t = \tau_{t-1} + \eta_t, \quad \tilde{X}_t = \Phi\tilde{X}_{t-1} + \tilde{U}_t, \tag{15}$$

with shocks vector i.i.d over time and distributed as

$$\begin{bmatrix} \eta_t \\ \tilde{U}_t \end{bmatrix} \sim \mathcal{N}\left(\mathbf{0}, \begin{bmatrix} \Omega_\eta & \mathbf{0}_{1\times K} \\ \mathbf{0}_{K\times 1} & \tilde{\Omega}_{K\times K} \end{bmatrix}\right). \tag{16}$$

Our estimation framework can be easily extended to allow for vector-valued $\boldsymbol{\tau}_t$, and we present such a general model in Appendix A. Letting $U_t \equiv \Gamma\eta_t + \tilde{U}_t$ and $Z_t = (\tau_t, X_t^\top)^\top$, the stochastic discount factor is

$$\begin{aligned} m_{t+1} =& -\delta_0 - \boldsymbol{\delta_1}^\top X_t - \frac{1}{2}\Lambda_t^\top\Lambda_t - \frac{1}{2}\Lambda_t^\top U_{t+1}, \quad \Lambda_t = \Sigma^{-1}(\Lambda_0 + \Lambda_1 Z_t), \\ \Omega \equiv& \mathbf{E}[U_t U_t^\top], \quad \Sigma\Sigma^\top = \Omega. \end{aligned} \tag{17}$$

Finally, the first column of Λ_1 is restricted to be $(I_K - \Phi)\Gamma$, so that the yields are affine in X_t instead of Z_t. In Appendix A, we show that

$$y_t^{(n)} = A_n + B_n^\top X_t, \tag{18}$$

where A_n and B_n satisfy the standard no-arbitrage recursions for zero-coupon yields.

The stochastic trend τ_t is unspanned by current yields, in the sense that the bond pricing equation (18) cannot be inverted to express τ_t as linear combinations of yields. However, τ_t

is useful for predicting future yields because

$$\mathbf{E}_t[X_{t+1}] = (I - \Phi)\underbrace{(\boldsymbol{\mu} + \Gamma\tau_t - X_t)}_{\text{coint. error}} + X_t. \tag{19}$$

The first term is the deviation from the cointegration trend. When the current state X_t is below the trend, it is expected to increase to catch up with the trend. For the same reason, τ_t is informative about expected excess bond returns controlling for X_t. Therefore, this formulation is essential for explaining the cointegration analysis in Section 2 and the excess bond return prediction regressions in Section 3.

4.1 Estimation

We estimate the model using two methods. Both methods treat X_t as observable and let it be the first five principal components of the $3, 4, \ldots, 240$-month yields. The yields are interpolated using the Svensson (1994) parameters estimated by Gürkaynak et al. (2007) and updated by the Federal Reserve Board.

The first method assumes that τ_t is observable. Following Bauer and Rudebusch (2020), we label it the "observed shifting endpoint" (OSE) model. Motivated by the statistical analysis in Section 2, our empirical proxy for τ_t is ∇y_t, the first principal component of the cumulative daily changes in the cross-section of Treasury zero-coupon yields during the FOMC windows. The results are quantitatively similar if we use changes during the FOMC window in individual yields, because all yields change by similar amounts during the FOMC windows (Figure 2). As Figure 3 shows, the first principal component of the FOMC-filtered yields accounts for 97% of their variations and closely follows the level factor of the unfiltered yields. The previous sections also show that ∇y_t well accounts for the common trend of Treasury yields and contains essential information on expected yields and term premia. Therefore, ∇y_t is a good summary of the downward trend of the yield curve over the past three decades. Our baseline estimation uses monthly observations. We let the daily changes in yields outside FOMC windows be zero and sum all the daily changes cumulatively over time. Then, we take the end-of-month values as our monthly observations of τ_t and the Treasury yields.

Given observed X_t and τ_t, we estimate the term structure model parameters using linear regressions à la Adrian et al. (2013). To account for τ_t and the unspanning-restriction (A4), we modify the regression equations and run a restricted OLS. The algorithm selects a set of excess bond returns and regresses them on the state vector Z_t and the estimated shocks V_t. Following Adrian et al. (2013), we select excess bond returns of the one-month holding period for maturities $n \in\{6, 12, 18, 24, 30, 36, 42, 48, 54, 60, 84, 120\}$ months. Appendix A describes the estimation procedures in detail. The linear regression approach requires no numerical optimization algorithms, making it much faster than the maximum likelihood approach in Bauer and Rudebusch (2020).

The second method assumes that τ_t is unobservable. This approach uses only Treasury yields data and does not attribute the trend to any observed variables. Following Bauer and Rudebusch (2020), we label this approach the "estimated shifting endpoint" (ESE) model. Although the model does not explicitly recognize monetary policy as the driver of τ_t, the trends generated by the ESE model are quite similar to those generated by the OSE model using ∇y_t as a proxy for τ_t. We proceed in two steps. First, we infer τ_t from observed X_t using the method in Section 2. Following Del Negro et al. (2017a) and Bauer and Rudebusch (2020), we specify a tight inverse-gamma prior for Ω_η with a mean of $6^2/1200$, which implies that the standard deviation of the change in τ_t over a century is 6 percentage points. Meanwhile, the Ω_η obtained from the $OSE : \nabla y_t$ model implies that the standard deviation of the change in τ_t over a century is 3 percentage points. Our prior is a conservative choice that limits the amount of yield variation attributed to the long-run trend, and the results are quantitatively similar if we use the value of Ω_η from the OSE model as the prior mean. Note that the unobserved trend model estimated here is Equation (15), and X_t consists of the first five principal components of the yields. Second, we treat the inferred $\hat{\tau}_t$ as the observed τ_t and estimate the model using the OSE method.

4.2 Estimates of Yield Trends

Section 2 established that ∇y_t is the cointegration trend for all yields. Now, we investigate this property in the context of our term structure model. The term structure model Equation (15) and the bond pricing equation (18) imply that the trend component of the n-yield is

$$y_t^{(n)*} \equiv \lim_{s\to\infty} \mathbf{E}_t[y_{t+s}^{(n)}] = A_n + B_n^\top \boldsymbol{\mu} + B_n^\top \Gamma \tau_t, \tag{20}$$

and the cyclical component is

$$\tilde{y}_t^{(n)} \equiv y_t^{(n)} - y_t^{(n)*} = B_n^\top \tilde{X}_t. \tag{21}$$

Figure 6 plots the observed monthly 10-year yield and $y_t^{(10)*}$ estimated from different models. We estimate the ESE model and the OSE models using separately ∇y_t, cumulative sums of ED1-ED4 shocks during 30-minute FOMC windows, or cumulative sums of changes in the federal funds target rate[6] on FOMC announcement dates as a proxy for τ_t. Note that the ESE approach only requires observed yields and infers the cointegration trend τ_t using statistical methods, so we can use it to check the validity of the empirical proxies for τ_t. The ESE trend closely fits the long-run decline in the 10-year yield. Meanwhile, the OSE: ∇y_t model using ∇y_t as an observable proxy for τ_t provides an estimate of $y_t^{(10)*}$ highly correlated with the ESE estimate. The model results corroborate that cumulative changes in Treasury yields during the time of FOMC announcements are a major factor in the secular decline in yields.

Changes in interest rate futures rates during 30-minute event windows around FOMC announcements are popular measures of monetary policy shocks in the literature. Section 2 demonstrated that the cumulative sums of the high-frequency monetary policy shocks trend downward and strongly correlate with ∇y_t. To strengthen the link between monetary policy and the downward common trend in Treasury yields, we use cumulative sums of high-frequency Eurodollar futures rates as empirical proxies for τ_t in the OSE model and report the estimated $y_t^{(10)*}$ in Figure 6. The labels ED1-ED4 correspond to the Eurodollar futures that expire in the current quarter or up to three quarters ahead. Each $y_t^{(10)*}$ series is estimated separately from the respective Eurodollar shocks. The four series are almost indistinguishable from each other and follow the same pattern as the $y_t^{(10)*}$ identified by the ESE or OSE:∇y_t model. Note that ∇y_t performed better than the Eurodollar shocks between 2009 and 2015 to fit the 10-year yield trend, as the Eurodollar shocks were essentially zero during the ZLB period, while long-term yields continued to decline. Since ∇y_t averages the changes in yields across all maturities, it captures the declines in long-term yields during the ZLB period. Overall, the trends identified by ∇y_t and the high-frequency Eurodollar shocks outside the ZLB period are very similar, confirming that monetary policy has been a key driver of secular interest rate trends over the last three decades.

In Figure 6, we also consider the federal funds target rate as an observable proxy for τ_t (OSE:FFR target). The $y_t^{(10)*}$ series implied by the federal funds target rate exhibits some downward trend and roughly follows the long-run pattern of the 10-year yield series, but the fit is much worse than the $y_t^{(10)*}$ series implied by other proxies for τ_t. The federal funds target rate dropped and then increased too much during the 2000s, whereas the long-maturity Treasury yields declined almost monotonically during that period. Although Piazzesi (2005) finds that the federal funds target rate helps an affine term structure model to match the observed yields, our results suggest that the high-frequency monetary policy shocks and ∇y_t are better at explaining the persistent variations in the yield curve.

Figure 6 about here.

[6]The data for the federal funds target rate are from Datastream.

We can compare the model-implied loadings of yields on ∇y_t to the regression coefficients of yields on ∇y_t in the data. We use ∇y_t as the observed proxy for τ_t and estimate the model using the OSE method. The model-implied loading on ∇y_t is $B_n^\top \Gamma$. Figure 6 plots these coefficients against maturities n. In the data, the coefficients are slightly larger than one, rising gradually from the short end, peaking at around the two-year maturity, and decreasing thereafter. The regression coefficient for the 10-year maturity corresponds to the value in the last column of Table 2. The model-implied loadings have similar patterns to their data counterparts and are contained in the 90% confidence intervals of the data estimates. To account for sampling uncertainty, we simulate 5,000 samples of τ_t and yields with the same length as the actual data and estimate the regression coefficients in each simulated sample. The 90% Monte Carlo interval of the regression coefficient contains the value obtained with the actual data and also contains the value 1 for all maturities. The latter fact suggests that our model-implied yield curve moves almost one-to-one with changes in monetary policy, and monetary policy mainly transmits via the conventional expectations component. Term premia barely load on the cumulative effects of monetary policy announcements.

Figure 7 about here.

4.3 Cumulative Changes in Expected Yields and Term Premia During FOMC Windows

The declines in yields around FOMC announcements could have been due to falling expectations of future policy rates, as suggested by standard linear new Keynesian models, or falling term premia. One possible mechanism for the decrease in term premiums could be "reaching for yield" by which yield-oriented investors purchase long-term bonds when short-term interest rates are reduced by monetary policy (Hanson and Stein (2015)). Other mechanisms include changes in liquidity premia (Drechsler et al. (2018), Lagos and Zhang (2020)), redistribution of wealth from risk-averse to risk-tolerant investors (Kekre and Lenel (2022)), or endogenous changes in investors' risk aversion (Pflueger and Rinaldi (2022)).

To quantify the cumulative effects of monetary on expected yields and risk premia, we decompose the yields using the OSE: ∇y_t model and apply the FOMC filter (Equation (1)) to each component. Hillenbrand (2021) finds that the term premia have declined by one to two percentage points around FOMC announcement dates using the Federal Reserve Board's stationary affine term structure models (Adrian et al. (2013), Kim and Wright (2005)). However, the stationary affine models assume that the yields follow a stationary AR(1) process, so the expected future yields have no stochastic trends by construction. The term premia, acting as residuals, must capture the declining trends of the yields. In Appendix C, we show that the original Adrian et al. (2013) model overestimates the declines in the 10-year term premium during FOMC windows than the OSE model.

Using the OSE model, we allow the expected yields to capture the declining trend and investigate whether the expected yields or the term premia have declined around FOMC announcement dates. We use the first principal component of cumulative yield changes around FOMC announcement dates, ∇y_t, as a proxy for τ_t. The data frequency is daily. We obtain the model-implied expected future short-term yields (risk-neutral yields) and term premia at the daily frequency and apply the filter defined by Equation (1) to each component.

To obtain model-implied yields at the daily frequency, we follow the procedures in Adrian et al. (2013). First, we estimate the model parameters using end-of-month data. Second, we compute the principal components of the daily yield curve, X_t, using weights computed from monthly data. Third, we combine A_n and B_n implied by the monthly estimation with daily X_t and τ_t to get the daily fitted yields and decompositions.

Figure 8 presents the risk-neutral and term premium components for the 5-, 7- and 10-year Treasury yields. For all yields, the secular declines over the whole sample are mainly attributable to declines in the risk-neutral component. Furthermore, the changes in the risk-neutral yields during the FOMC windows account for substantial parts of the secular declines in the risk-neutral yields. The 5-year risk-neutral yield decreased by 8.5 percentage points in the full sample and by 4.6 percentage points during the FOMC windows (4.6/8.5=54%). The 10-year risk-neutral yield decreased by 7.5 percentage points over the entire sample period and by 5.2 percentage points during FOMC windows (5.2/7.5 = 69%). On the other hand, the term premia are much less responsive to monetary policy. For example, the 10-year term premia decreased by 1.4 percentage points in the whole sample and by 2 percentage points during the FOMC windows. Interestingly, term premia decreased more during FOMC windows than in the whole sample, indicating that term premia bounced up significantly between FOMC meetings.

Figure 8 about here.

To investigate the effects of monetary policy on risk-neutral yields and term premia more rigorously, we follow the high-frequency identification literature to regress the two components of the yield curve on high-frequency monetary policy shocks. The dependent variables are the daily changes on the announcement date or the changes over the three-day event windows in the risk-neutral yields and term premia. The independent variable is the first principal component of ED1-ED4 high-frequency shocks (MPS) or the orthogonalized monetary policy shock constructed by Bauer and Swanson (2022b), eliminating the puzzling "Fed information effect" (MPS_ORTH). Table 7 reports the responses of the 5- and 10-year term premia and risk-neutral yields to the shocks. Although the monetary policy shock has statistically significant effects on both components, the effects on risk-neutral yields are much larger. Therefore, the regression results are consistent with the time series plots showing that the secular declines in yields during FOMC announcement windows are primarily due to reductions in short-rate expectations.

Table 7 about here.

4.4 Model-Implied Excess Bond Return Prediction

Section 3 established that ∇y_t has significant predictive power for excess bond returns, which is not spanned by linear combinations of yields. We replicate this result with our shifting-endpoint term structure models. We simulate 5,000 artificial samples from each of the following three models: the stationary Adrian et al. (2013) model (FE), the shifting-endpoint model using ∇y_t as the observed proxy for τ_t (OSE), and the shifting-endpoint model using estimated τ_t (ESE). We estimate Equation (11) with and without τ_t as a predictor using the simulated data and report the means and the 2.5^{th} and 97.5^{th} percentiles of the resulting R^2.

Table 8 reports the R^2 for predicting the excess bond returns of the 1-year holding period from actual and simulated data. The top row reports the R^2 for regressions using actual data with and without ∇y_t as a predictor in addition to the principal components of observed yields, reproducing columns (1) and (6) of Table 3. Column (3) of Table 3 shows that including ∇y_t more than doubles the R^2.

The remaining rows of Table 8 report the R^2 produced by different models. For the F.E. model, ∇y_t provides essentially no gains in predictive power for the simulated excess bond returns. This is natural because the yields generated by the F.E. model are spanned by the principal components, and the model assumes no trend in the state variables.

For the OSE model, ∇y_t provides substantial gains in predictive power. The mean increase in R^2 is 19 percentage points, and the actual increase in R^2 (29 percentage points) is contained in the 95% Monte Carlo interval. The ESE model produces similar results. The gain in R^2 implied by the ESE model is smaller than that implied by the OSE model, but the 95% Monte Carlo interval for the former also contains the actual data. The shifting-endpoint models replicate the large predictive gains from adding τ_t in excess bond returns predictions, and explicitly attributing τ_t to monetary policy appears to perform better than estimating τ_t from observed yields.

In Table A4, we show that using ∇y_t as a proxy for τ_t in the OSE model also helps forecast Treasury yields out-of-sample, and the performances at long horizons beat the random walk.

Table 8 about here.

Why does the trend provide additional predictive power? We can obtain intuitions from the analytical expression of excess returns in the shifting-endpoint term structure model. Starting from the no-arbitrage condition $1 = \mathbf{E}_t\left[\exp\left\{m_{t+1} + rx_{t+1}^{(n)} + y_t^{(1)}\right\}\right]$, one can show that[7]

$$\mathbf{E}_t\left[rx_{t+1}^{(n)}\right] = const + \boldsymbol{\beta}^{(n)\top}(\Lambda_0 + \Lambda_{11}\tau_t + \Lambda_{12}X_t), \tag{22}$$

where Λ_{11} and Λ_{12} are the first and the rest columns of Λ_1. Appendix A shows the details of the derivation. The terms in parentheses are proportional to the price of risk, $\Lambda_t = \Omega^{-\frac{1}{2}}(\Lambda_0 + \Lambda_1 Z_t)$, which determines the time-varying risk premia. The presence of τ_t in parentheses implies that monetary policy can affect bond yields by changing the term premia, which is confirmed by empirical studies (for example, Pflueger and Rinaldi (2022)). Since our model imposes $\Lambda_{11} = (I_K - \Phi)\Gamma$ for τ_t to be unspanned, the coefficient on τ_t in Equation (22) is nonzero.

5 A Taylor-Rule Interpretation?

Monetary policy reacts to macroeconomic conditions. For example, the standard Taylor rule stipulates that the policy interest rate is a linear combination of inflation and the output gap, plus an unexpected "monetary policy shock". In this case, if the monetary policy shocks are absent or inconsequential, the monetary policy trend ∇y_t is essentially a linear combination of inflation and output trends. Our main argument about the driver of the secular trend in Treasury yields is equivalent to the classical inflation- or output-driven mechanisms for the interest rate trend. That is, the secular declines in interest rates over the last three decades were ultimately driven by a decreasing inflation trend or a productivity slowdown. To rule out this possibility, we proceed in two steps. First, we test whether a linear combination of inflation and output trends has a predictive performance similar to ∇y_t. Second, we estimate an OSE dynamic term structure model using inflation and real output trends as proxies for $\boldsymbol{\tau}_t$ and compare the model-implied interest rate trends with those implied by ∇y_t.

[7] The derivations follow Adrian et al. (2013). One needs to assume $\boldsymbol{\beta}^{(n)\top} = \boldsymbol{\beta}_t^{(n)\top} \equiv \mathbf{Cov}_t\left(rx_{t+1}^{(n)}, U_{t+1}\right)\Omega^{-1}$ and $\boldsymbol{\gamma}^{(n)\top} = \boldsymbol{\gamma}_t^{(n)\top} \equiv \mathbf{Cov}_t\left(rx_{t+1}^{(n)}, V_{t+1}\right)\Omega_V^{-1}$, that is, the conditional covariances are constant.

5.1 Predicting Excess Bond Returns

We run the regression

$$\overline{rx}_{t+1} = \alpha + \boldsymbol{PC}_t^\top \boldsymbol{\beta} + \boldsymbol{\tau}_t^\top \boldsymbol{\gamma} + \varepsilon_{t+1}, \tag{23}$$

where $\boldsymbol{\tau}_t$ is a vector of the inflation trend and output factor. For the output factor, we consider the 2-sided real output growth trend or the output gap estimated by Laubach and Williams (2003). Table 9 reports regression results for the annual holding period[8]. Compared with inflation and output trends, ∇y_t provides the largest improvement in R^2 and is highly significant. The output factors are not significant for predicting excess bond returns. The coefficient on output gap x_t^* is positive, though the Taylor rule stipulates that the policy interest rate should respond positively to the output gap, and thus the coefficients on π_t^* and x_t^* should be both negative. This suggests that the cointegration trend for the yield curve is not merely the policy rate's response to the persistent variations in inflation and output. Therefore, ∇y_t is not equivalent to a linear combination of inflation and output factors. Monetary policy has unique roles in determining the secular trend in Treasury yields, which is consistent with the similarity between the cumulative sums of *unexpected* monetary policy shocks and ∇y_t presented in Figure 4.

Table 9 about here.

5.2 Model-Implied Interest Rate Trends

We let $(\pi_t^*, g_t^*)^\top$ or $(\pi_t^*, x_t^*)^\top$ be the empirical proxies for the 2×1-dimensional trend vector $\boldsymbol{\tau}_t$, where π_t^* is the inflation trend, g_t^* is the real output growth trend, and x_t^* is the output gap. The latter two series are borrowed from the 2-sided estimates in Laubach and Williams (2003). The state dynamics and SDF are the same as the baseline model, except that the trend is a vector here. We estimate the dynamic term structure model using the OSE method and study the model-implied trend for the 10-year yield. Due to the availability of the macroeconomic series, the model is estimated at the quarterly frequency.

Figure 9 shows the estimated trend for the 10-year yield using the ESE model and the OSE model with different proxies for $\boldsymbol{\tau}_t$. As the monthly estimates in Figure 6, the ESE-implied trend fits the observed series very well, and the OSE-implied trend proxied by ∇y_t is quite close to the ESE-implied trend. The trends proxied by macroeconomic variables fit much worse. Both trends start lower than the observed 10-year yield by about 1 percentage point and end higher by about 1 percentage point. Therefore, using inflation and output

[8]We find similar results for the quarterly holding period, which are reported in Table A3

trends to proxy $\boldsymbol{\tau}_t$, the model underestimates the secular decline in the 10-year yield by 2 percentage points.

In summary, although inflation and output trends capture substantial fractions of interest rate trends, the explanatory power is outperformed by the cumulative effects of monetary policy. Monetary policy uniquely determines the secular trend in interest rates, going above and beyond reacting to macroeconomic factors.

Figure 9 about here.

6 Conclusion

This paper shows that monetary policy has persistent and profound impacts on the Treasury yield curve. We provide new evidence that Treasury yields and the cumulative effects of monetary policy are cointegrated and that monetary policy explains the persistent variations in Treasury yields. Deviations in yields relative to the trend of monetary policy are consequential in predicting future yields and excess bond premia, and observed yields do not span this factor. We build a dynamic term structure with a stochastic trend to explain the empirical facts. The model implies that monetary policy mainly affected expected short-term interest rates before the 2008 financial crisis and significantly reduced term premia during the zero-lower-bound episode. Ignoring the stochastic trend, as standard affine term structure models do, would significantly underestimate the effects of monetary policy on expected interest rates. To this end, our model provides stronger support for the implications of standard new Keynesian models relative to existing models of interest rates. Our analysis of the effects of monetary policy on term premia during the ZLB episode is also consistent with the views of intermediary asset pricing models.

Nonlinear new Keynesian asset pricing models typically imply that monetary policy shocks significantly affect term premia. For example, Pflueger and Rinaldi (2022) find that the effects of monetary policy shocks on term premia and risk-neutral yields have similar magnitudes, with the former even larger than the latter. These implications are in stark contrast to the empirical findings in this paper. One possible reason is that the new Keynesian models are stationary, and thus, the long-maturity risk-neutral yields must have minimal variations. It is interesting to incorporate persistent stochastic trends in new Keynesian asset pricing models and reconcile the difference from affine term structure models, which we leave for future research.

Figure 1: FOMC announcement dates and Treasury yields.

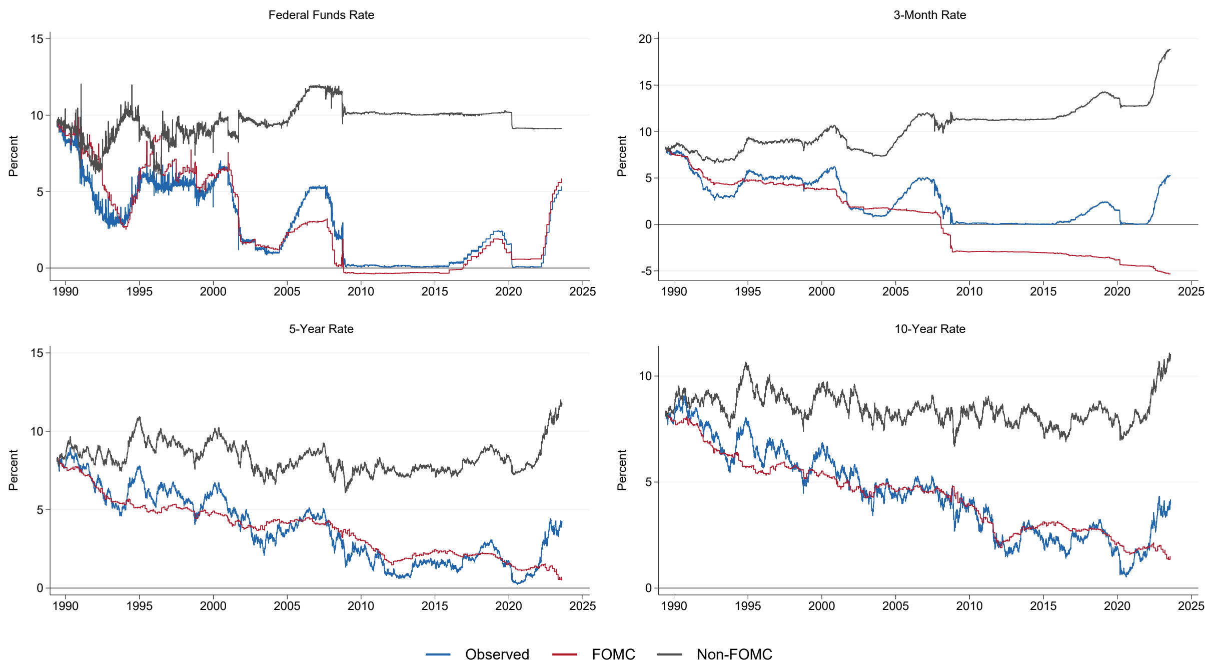

Notes: Comparing observed yields with their cumulative changes in or out of FOMC windows. Each FOMC window ranges from the day before to the day after an FOMC announcement date.

Figure 2: Cumulative yield changes during FOMC announcement windows.

Notes: The top panel collects cumulative yield changes during FOMC announcement windows for different maturities. The procedures for constructing the series are described by Equation (1). The bottom panel plots the observed yields.

Figure 3: FOMC announcement dates and Treasury yields: principal components.

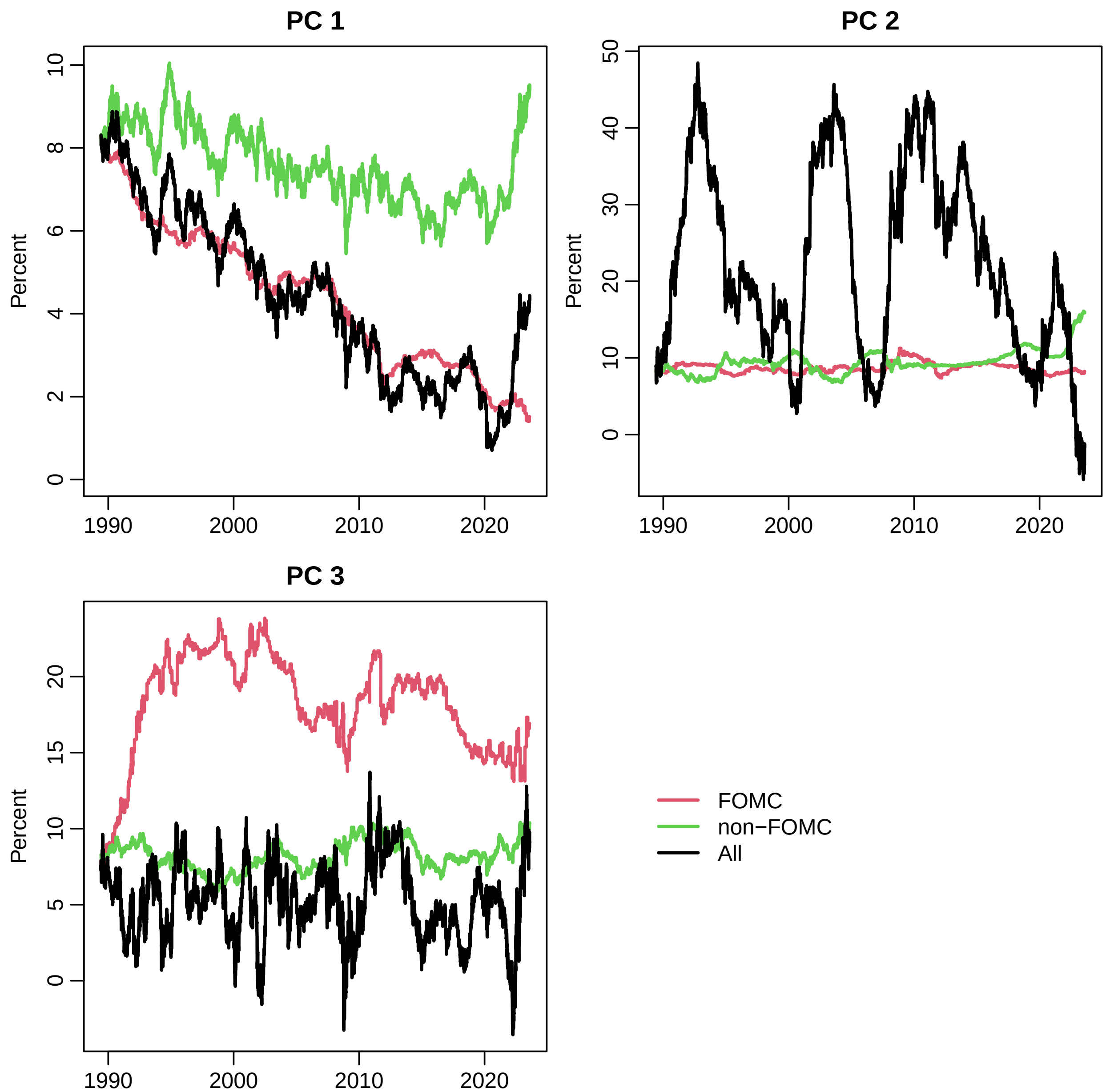

Notes: The first three principal components of the nominal Treasury yield curve and yield changes during or outside the FOMC window. The weighting matrix is normalized such that each principal component's weights on all yields sum to 1. The percentages of total variations explained by the first three principal components are 94.26, 5.34, and 0.24 for the unfiltered yield curve; 96.96, 2.93, and 0.08 for the cumulative changes during the FOMC window; 62.30, 31.90, and 4.18 for the cumulative changes outside the FOMC window.

Figure 4: Cumulative yield changes and monetary policy shocks.

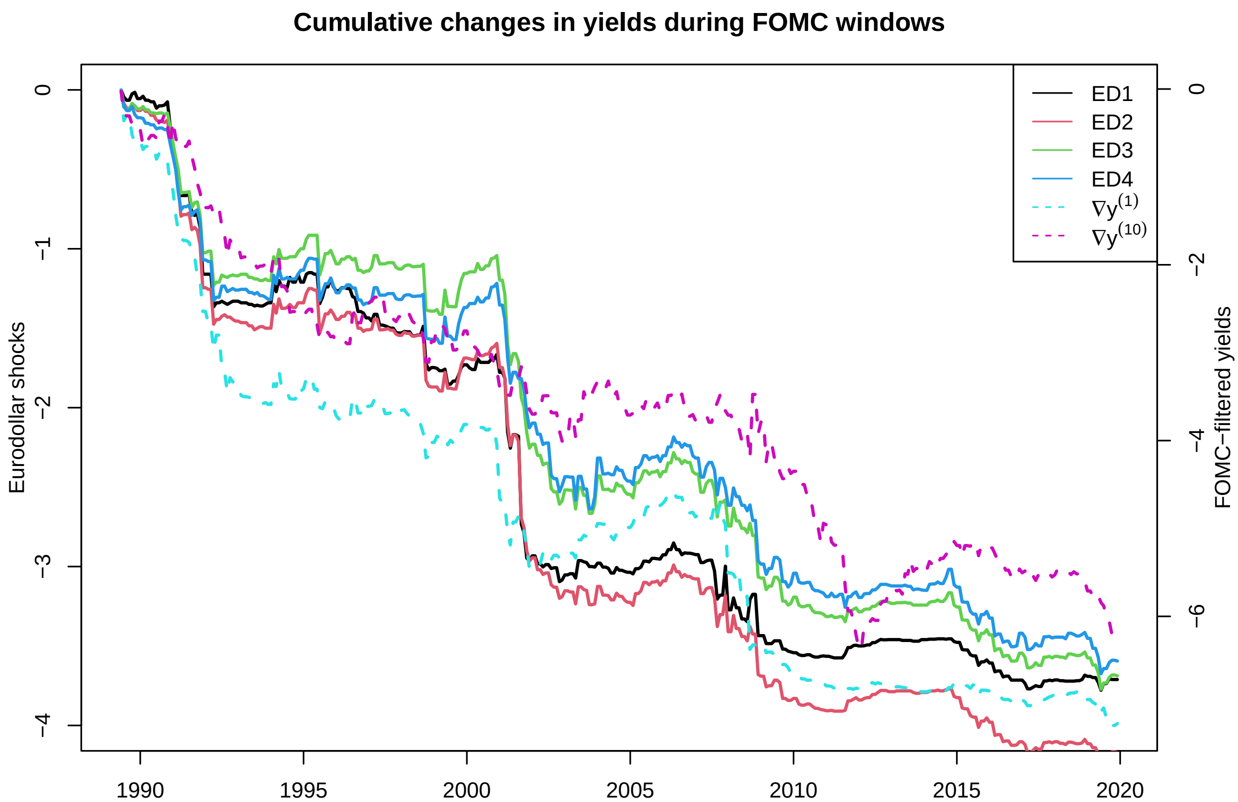

Notes: The monetary policy shocks (left axis) are changes in the first four Eurodollar futures (ED1-ED4) rates during 30-min FOMC press release windows. The FOMC-filtered yields (right axis) are daily changes in Treasury yields during the FOMC windows; see Equation (1). The monetary policy shocks and daily yield changes are summed cumulatively, setting values on non-FOMC days to zero. Finally, we take the last observations of each month.

Figure 5: Treasury yields and trends: with yield-specific trends.

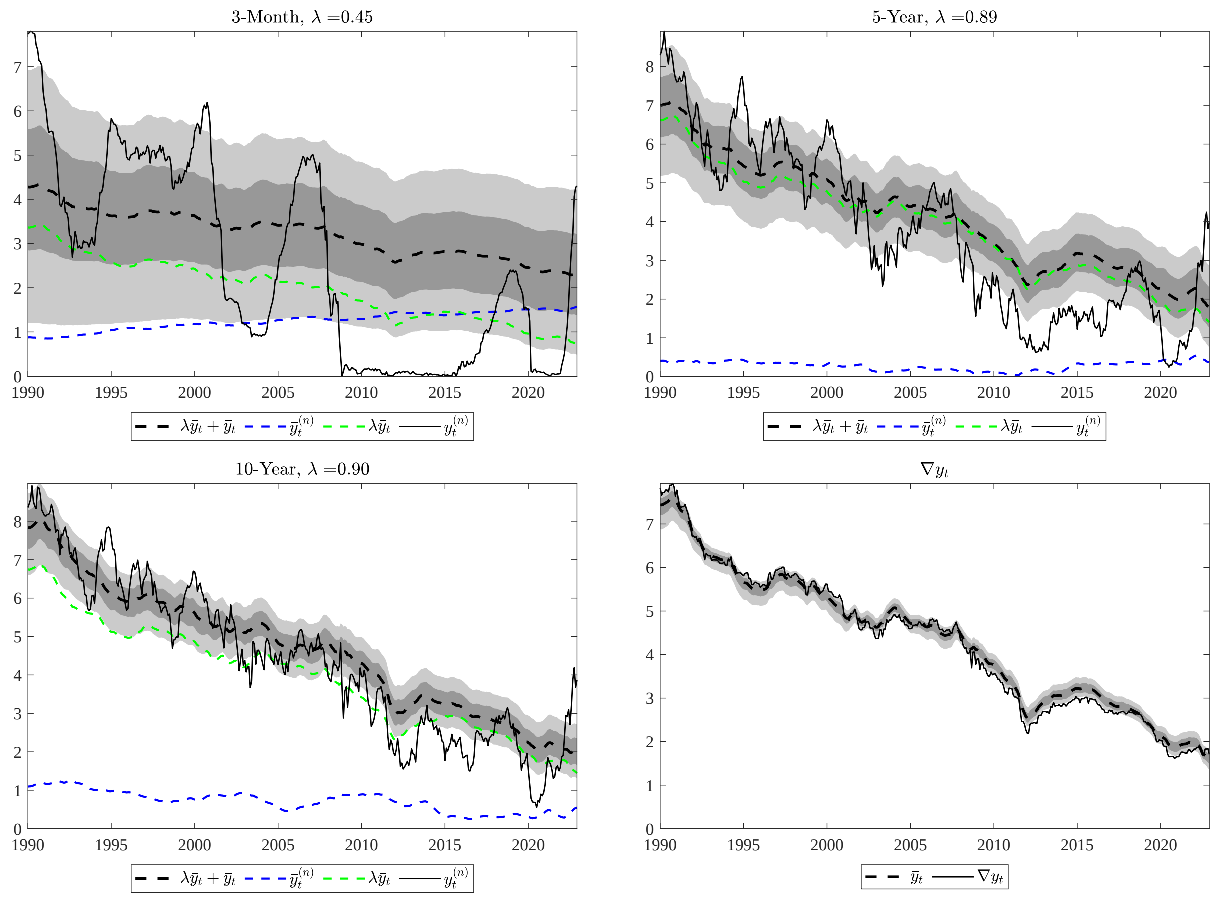

Notes: Each yield $y_t^{(n)}$ is decomposed as $y_t^{(n)} = \lambda^{(n)}\bar{y}_t + \bar{y}_t^{(n)} + \tilde{y}_t^{(n)}$, where $\lambda^{(n)}$ is a yield-specific loading on the common trend, $\bar{y}_t = \bar{y}_{t-1} + \eta_t$ is a stochastic trend common to all yields, $\bar{y}_t^{(n)} = \bar{y}_t^{(n)} + \eta_t^{(n)}$ is a yield-specific stochastic trend, and $\tilde{y}_t^{(n)}$ is an element of a stationary VAR component. We include $n = 0.25, 5$ and 10 years in the exercise. We also include ∇y_t, the first principal component of the FOMC-filtered yields, and decompose it as $\nabla y_t = \bar{y}_t + \tilde{y}_t^{FOMC}$. Note that $y_t^{(n)}$ and ∇y_t share the same stochastic trend $\bar{y}_t$, but ∇y_t has a unitary loading on $\bar{y}_t$. Median estimates of $\lambda^{(n)}$ are presented in the titles, and the plots show the median estimates of the trends together with the 95% confidence band of the overall trend for each yield.

Figure 6: Observed 10-year yield and its trend component implied by different models.

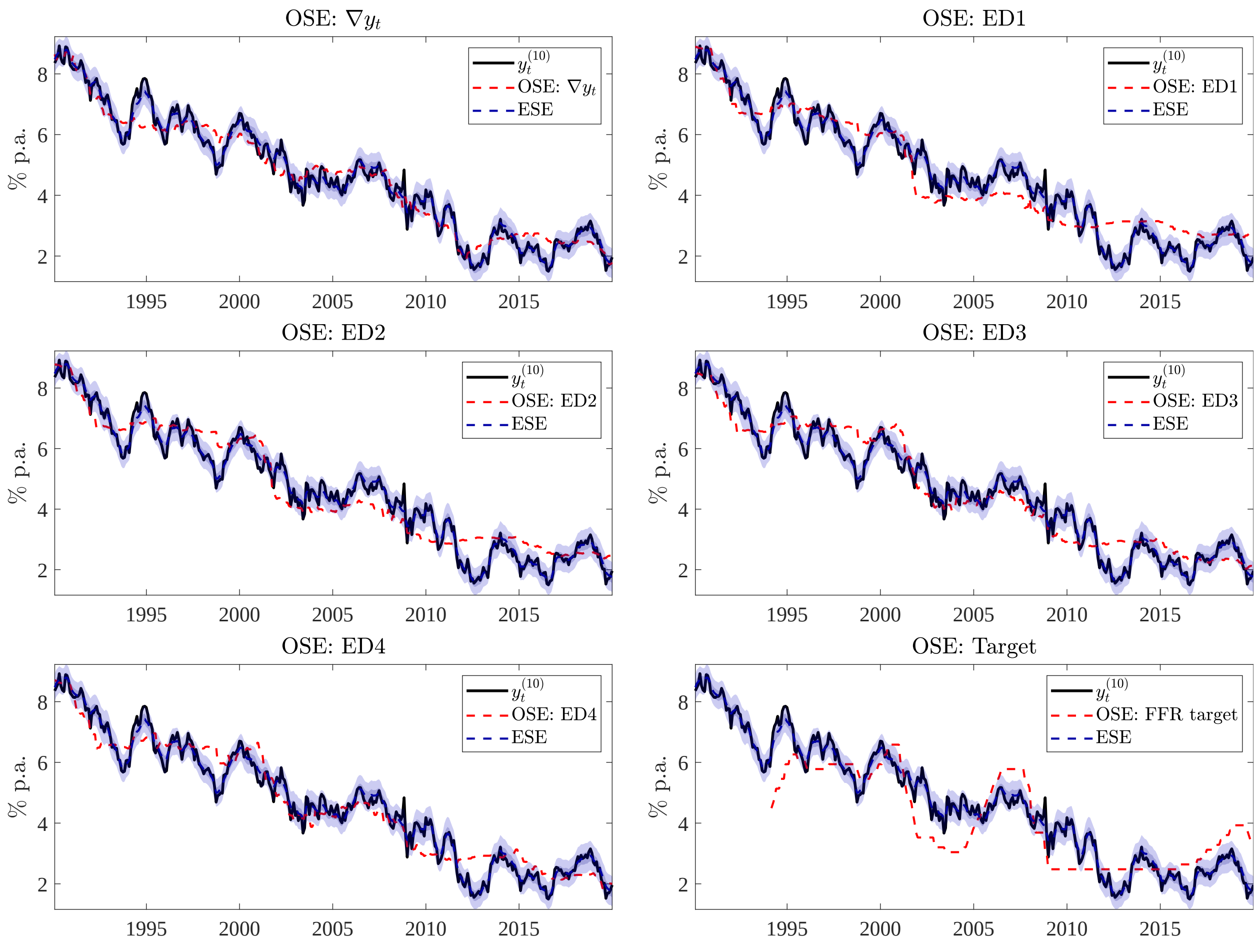

Notes: This figure compares the trends for the ten-year Treasury yield estimated from different measures of monetary policy shocks. The trend component is estimated using either the OSE or the ESE approach, defined as $y_t^{(10)*} = A_{10} + B_{10}^{\top}(\mu + \Gamma\tau_t)$ using the model parameters A, B and proxy/estimate of τ_t. The solid curve is the observed 10-year Treasury yield. The red dashed curve is estimated from the OSE model using different monetary policy trends to proxy τ_t. The blue dashed line is estimated from the ESE model. The shaded areas are the 68% and 99% confidence intervals.

Figure 7: Loadings of yields on the cumulative effects of monetary policy announcements.

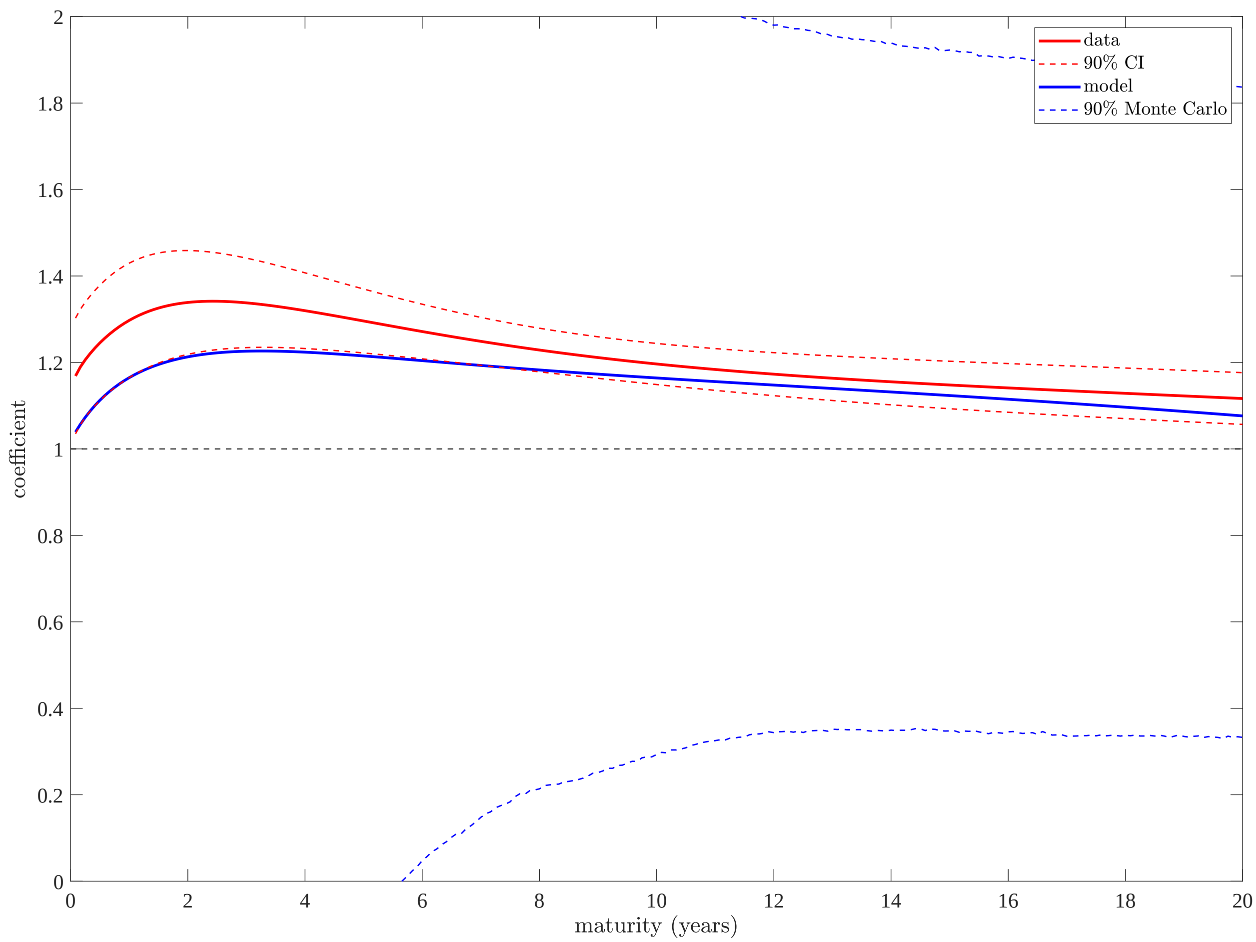

Notes: Comparison of loadings of Treasury yields on ∇y_t in the data and in the OSE dynamic term structure model. Data: slope coefficients for $y_t^{(n)} = \alpha + \beta \nabla y_t + u_t$ for each maturity, estimated using the dynamic OLS regression method in Stock and Watson (1993). Model: the solid line is $B_n^\top \Gamma$. The dashed lines are the 90% confidence intervals (data) or Monte Carlo intervals (model) for regression coefficients in samples with the same length as the data simulated from an OSE model.

Figure 8: Filtering the yield curve components.

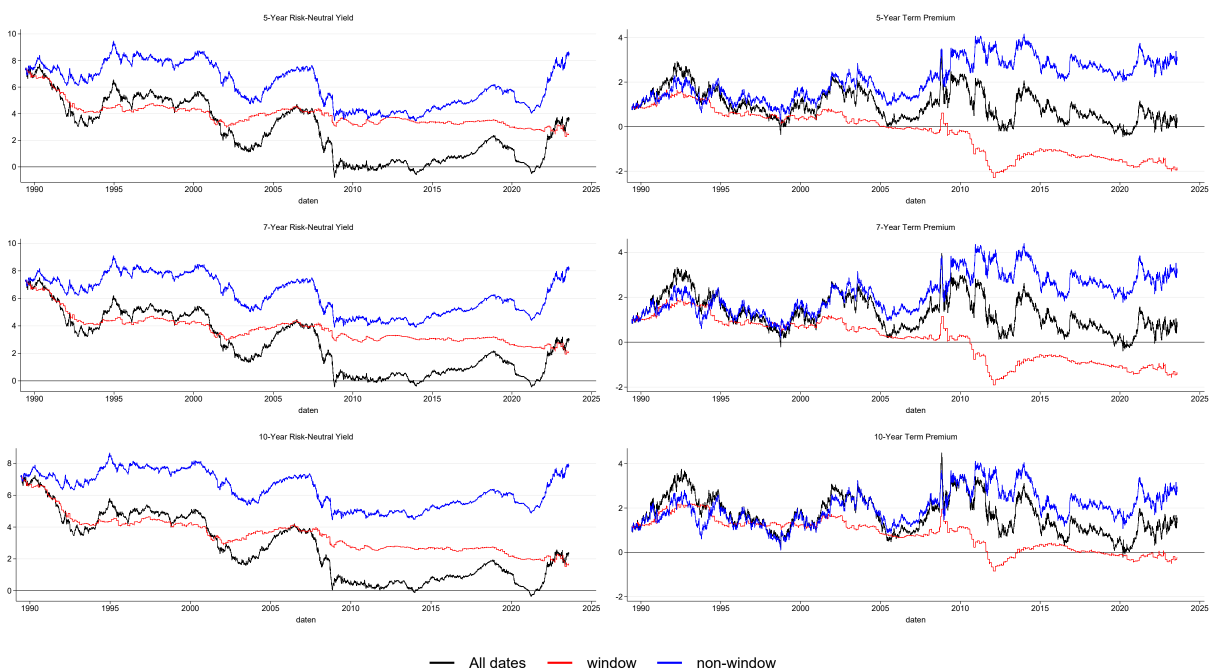

Notes: This figure filters the risk-neutral and term premium components of long-term yields using Equation (1). The risk-neutral and term premium components are estimated using the OSE model, and the first principal component of FOMC-window yields serves as the trend τ_t.

Figure 9: Trends for the 10-year yield: macro vs. monetary policy

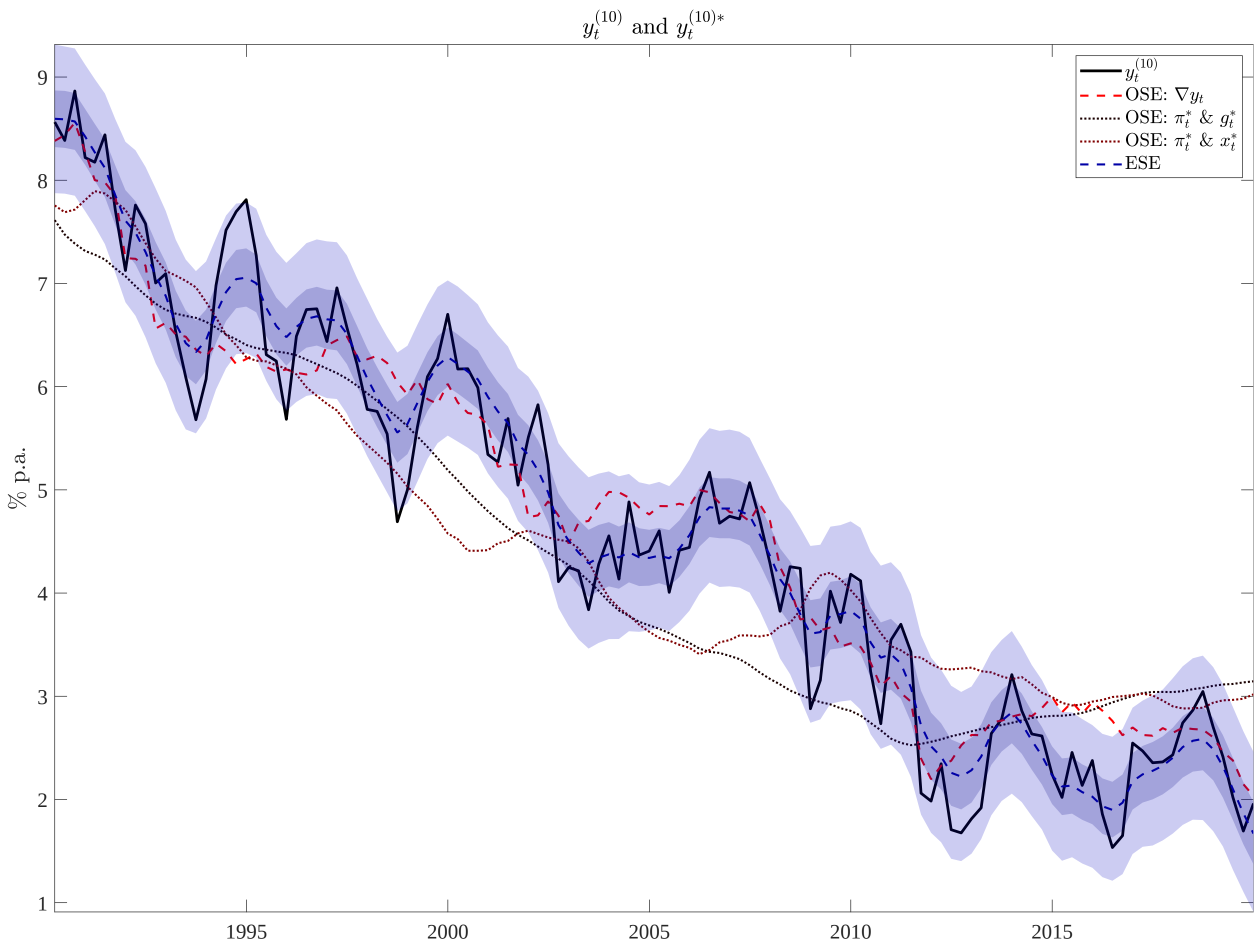

Note: This figure compares the trends for the ten-year Treasury yield estimated from macroeconomic trends or ∇y_t. The solid curve is the observed 10-year Treasury yield. The trend is $y_t^{(10)*} = A_{10} + B_{10}^{\top}(\mu + \Gamma\boldsymbol{\tau}_t)$ using the model parameters A, B and the empirical proxy for $\boldsymbol{\tau}_t$. The red dashed curve is estimated using ∇y_t to proxy τ_t in the OSE model. The dotted curves are estimated using inflation and output growth trend (g_t^*) or output gap (x_t^*) as proxies for $\boldsymbol{\tau}_t$ in the OSE model. The macroeconomic trend variables are the 2-sided estimates from Laubach and Williams (2003). The blue dashed line is estimated from the ESE model. The shaded areas are the 68% and 99% confidence intervals.

Table 1: Summary statistics of Eurodollar futures shocks.

	count	mean	sd	min	max
ED1	254	-0.01	0.06	-0.55	0.18
ED2	254	-0.01	0.06	-0.48	0.15
ED3	254	-0.01	0.06	-0.31	0.18
ED4	254	-0.01	0.06	-0.27	0.24
1-year yield	254	-0.03	0.11	-0.61	0.26
10-year yield	254	-0.02	0.13	-0.45	0.72

Notes: ED1-ED4 denote 30-min Eurodollar futures shocks. "1-year yield" and "10-year yield" are changes in the respective yield from the day before the FOMC announcement date to the day after. All variables are summed within each month.

Table 2: Cointegration tests for the 10-year yield and macroeconomic trends.

	$y_t^{(10)}$	$\nabla y_t^{(10),non-FOMC}$	(1)	(2)	(3)	(4)	(5)	(6)
constant	4.78	8.48	-1.06	-1.18	-3.19	-1.63	-3.26	-1.17
	(0.45)	(0.13)	(1.56)	(0.52)	(0.45)	(0.43)	(0.33)	(0.27)
π_t^*			2.39	1.56	2.05	1.86		
			(0.65)	(0.23)	(0.17)	(0.18)		
r_t^*				1.23	1.94	1.31		
				(0.13)	(0.11)	(0.09)		
i_t^*							2.03	
							(0.08)	
∇y_t								1.27
								(0.07)
R^2			0.54	0.91	0.94	0.94	0.94	0.91
Memo: r^*				filtered	real-time	mov. avg.	real-time	
SD	1.92	0.67	1.24	0.62	0.57	0.65	0.57	0.53
$\hat{\rho}$	0.95	0.77	0.91	0.70	0.60	0.70	0.60	0.64
Half-life	12.6	2.6	7.2	2.0	1.4	1.9	1.4	1.5
ADF	-1.92	-3.87***	-1.51	-4.38**	-4.67***	-2.87	-4.63***	-5.16***
PP	-4.06	-26.92***	-7.80	-34.03**	-36.36***	-24.30*	-35.80***	-39.91***
LFST	0.00	0.00	0.00	0.42	0.34	0.33	0.25	0.89
Johansen $r = 0$			25.64***	45.99***	68.06***	66.22***	47.93***	30.30***
Johansen $r = 1$			3.29	18.46*	30.30***	27.65***	11.98**	8.80*
ECM $\hat{\alpha}$			-0.06	-0.28	-0.46	-0.60	-0.44	-0.46
			(0.03)	(0.08)	(0.14)	(0.15)	(0.14)	(0.11)

Notes: * $p < 0.1$, ** $p < 0.05$, *** $p < 0.01$. Dynamic OLS regressions of the 10-year yield on macroeconomic trends, including four leads and lags of the yield and differenced trend variables. Newey-West standard errors with 6 lags are in parentheses. The estimates of $\pi_t t^*$ and r_t^* are from Bauer and Rudebusch (2020) and i_t^* is the sum of π_t^* and the real-time r_t^*. ∇y_t is the first principal component of cumulative changes in all Treasury yields during FOMC windows. The second panel reports statistics for the cointegration residuals, including standard deviations (SD), first-order autocorrelation coefficients ($\hat{\rho}$), half-lives ($\ln(0.5)/\ln(\hat{\rho})$), Augmented Dickey-Fuller (ADF) and Phillips-Perron (PP) unit root test statistics, and p-values for Müller-Watson low-frequency stationary test (LFST). The third panel reports statistics for an error-correction model for first differences of the yield and each macroeconomic trend. The model includes four lags and a constant. The statistics reported are the Johansen trace statistic for the cointegration rank (r) among the yield and macroceconomic trend against the alternative that the rank exceeds the specified level, and the loading of the differenced yield on the cointegrated variable (ECM $\hat{\alpha}$).

Table 3: Predicting excess bond returns.

	(1)	(2)	(3)	(4)	(5)	(6)	(7)
				Panel A: Full sample, 1989-2018			
PC1	0.46	1.38	4.20	6.47	5.76	6.86	7.33
	(0.27)	(0.45)	(0.95)	(1.30)	(1.11)	(1.16)	(1.21)
PC2	1.10	1.38	1.61	1.92	1.91	1.68	1.82
	(0.33)	(0.24)	(0.20)	(0.17)	(0.18)	(0.20)	(0.18)
PC3	-2.28	-1.78	0.58	3.53	2.63	1.11	1.98
	(2.13)	(2.15)	(2.18)	(2.69)	(2.25)	(2.07)	(2.27)
π_t^*		-4.20	-7.61	-11.19			
		(1.84)	(2.09)	(2.30)			
		[0.28]	[0.10]	[0.04]			
r_t^*			-5.06	-14.00			
			(1.64)	(3.84)			
			[0.12]	[0.15]			
i_t^*					-11.19		-3.27
					(2.42)		(2.38)
					[0.05]		[0.41]
∇y_t						-9.17	-7.63
						(1.63)	(1.96)
						[0.02]	[0.03]
R^2	0.23	0.28	0.38	0.44	0.43	0.52	0.53
Memo: r^*			filtered	real-time	real-time		real-time
				Panel B: Subsample, 1994-2018			
PC1	0.86	1.18	4.10	5.69	5.64	6.24	7.45
	(0.31)	(0.46)	(0.71)	(1.09)	(1.02)	(0.77)	(0.94)
PC2	1.33	1.43	1.68	1.92	1.93	1.64	1.86
	(0.33)	(0.30)	(0.23)	(0.22)	(0.21)	(0.21)	(0.18)
PC3	-1.84	-2.08	-0.29	2.43	2.22	0.41	1.90
	(2.31)	(2.28)	(2.15)	(2.72)	(2.31)	(1.99)	(2.27)
π_t^*		-3.32	-10.40	-10.99			
		(3.01)	(2.91)	(2.97)			
		[0.60]	[0.12]	[0.14]			
r_t^*			-4.83	-12.04			
			(1.24)	(3.34)			
			[0.07]	[0.26]			
i_t^*					-11.66		-5.59
					(2.47)		(2.79)
					[0.09]		[0.30]
∇y_t						-8.66	-6.91
						(1.21)	(1.52)
						[0.01]	[0.03]
R^2	0.30	0.31	0.41	0.46	0.45	0.54	0.56
Memo: r^*			filtered	real-time	real-time		real-time

Notes: Predictive regressions for annual average excess bond returns $\overline{rx}_{t+1} \equiv \frac{1}{14}\sum_{n=2}^{15} rx_{t+1}^{(n)}$. The independent variables are the first three principal components of yields (PC1, PC2, PC3), estimates of the inflation trend π_t^*, the real-rate trend r_t^*, and the long-run nominal short rate i_t^*, and the first principal component of cumulative changes in yields during the FOMC window ∇y_t. The numbers in parentheses are Newey-West standard errors and in square brackets are small-sample p values à la Bauer and Hamilton (2018).

Table 4: Predicting excess bond returns: no principal components.

	(1)	(2)	(3)	(4)	(5)	(6)
			Panel A: Full sample, 1989-2018			
π_t^*	0.73	0.80	0.61			
	(1.48)	(1.73)	(1.75)			
r_t^*		-0.08	0.27			
		(1.05)	(1.66)			
i_t^*				0.44		
				(0.81)		
∇y_t					0.10	
					(0.58)	
R^2	0.00	0.00	0.01	0.00	0.00	
Memo: r^*		filtered	real-time	real-time		
			Panel B: Subsample, 1994-2018			
π_t^*	3.52	3.66	3.60			
	(2.50)	(2.76)	(2.95)			
r_t^*		-0.15	-0.10			
		(1.05)	(1.71)			
i_t^*				0.80		
				(1.09)		
∇y_t					0.15	
					(0.78)	
R^2	0.02	0.03	0.02	0.01	0.00	
Memo: r^*		filtered	real-time	real-time		

Notes: Predictive regressions for annual average excess bond returns $\overline{rx}_{t+1} \equiv \frac{1}{14}\sum_{n=2}^{15} rx_{t+1}^{(n)}$. The independent variables are the estimates of the inflation trend π_t^*, the real-rate trend r_t^*, and the long-run nominal short rate i_t^*, and the first principal component of cumulative changes in yields during the FOMC window ∇y_t. Numbers in parentheses are Newey-West standard errors.

Table 5: Predicting bond excess Returns: detrended yields.

	(1)	(2)	(3)	(4)	(5)	(6)	(7)
			Panel A: Full sample, 1989-2018				
PC1	0.58	0.31	1.39	1.22	0.47	2.25	2.08
	(0.34)	(0.53)	(0.67)	(0.79)	(0.80)	(0.55)	(0.72)
PC2	1.34	1.37	1.37	1.50	1.84	1.76	0.17
	(0.33)	(0.29)	(0.33)	(0.34)	(0.23)	(0.21)	(0.28)
PC3	-1.85	-2.22	-0.80	0.88	2.69	0.53	5.34
	(2.27)	(2.27)	(2.40)	(3.00)	(2.44)	(1.92)	(0.65)
R^2	0.30	0.29	0.33	0.36	0.45	0.54	0.49
Trend		π_t^*	r_t^*	r_t^*	i_t^*	∇y_t	
Memo: r^*			filtered	real-time	real-time		
			Panel B: Subsample, 1994-2018				
PC1	0.46	0.57	1.32	1.06	0.62	1.84	2.33
	(0.27)	(0.51)	(0.56)	(0.63)	(0.81)	(0.81)	(0.74)
PC2	1.10	1.39	1.10	1.12	1.83	1.79	0.04
	(0.33)	(0.24)	(0.33)	(0.34)	(0.21)	(0.18)	(0.26)
PC3	-2.28	-1.83	-1.53	-1.38	2.77	1.22	6.12
	(2.13)	(2.15)	(2.36)	(2.72)	(2.13)	(1.96)	(0.77)
R^2	0.23	0.28	0.25	0.24	0.42	0.52	0.53
Trend		π_t^*	r_t^*	r_t^*	i_t^*	∇y_t	
Memo: r^*			filtered	real-time	real-time		

Notes: Predictive regressions for annual average excess bond returns $\overline{rx}_{t+1} \equiv \frac{1}{14}\sum_{n=2}^{15} rx_{t+1}^{(n)}$. In specification (1), the independent variables are the first three principal components of observed 1- to 15-year yields. In specifications (2)-(6), the independent variables are the first three principal components of the residuals in the regressions for yields on the respective trend variables indicated in the last row. In specification (7), the independent variables are the first three principal components of changes in the 1- to 15-year yields outside the FOMC windows. π_t^* is the trend inflation, i_t^* is the long-run nominal short rate in Bauer and Rudebusch (2020), and ∇y_t is the first principal component of the cumulative daily changes in the cross-section of Treasury zero coupon yields during FOMC announcement windows. Newey-West standard errors with six lags are in the parentheses.

Table 6: Predicting excess bond returns: orthogonalized trends.

	(1)	(2)	(3)	(4)	(5)
		Panel A: Full sample, 1989-2018			
π_t^*	-3.46	-6.06	-9.13		
	(2.77)	(2.78)	(2.72)		
r_t^*		-4.32	-11.46		
		(2.08)	(4.24)		
i_t^*				-9.29	
				(2.77)	
∇y_t					-8.95
					(2.01)
R^2	0.02	0.07	0.10	0.09	0.20
Memo: r^*		filtered	real-time	real-time	
		Panel B: Subsample, 1994-2018			
π_t^*	-1.09	-6.53	-7.12		
	(4.47)	(5.23)	(3.78)		
r_t^*		-3.64	-9.85		
		(1.92)	(4.06)		
i_t^*				-8.94	
				(3.04)	
∇y_t					-8.45
					(1.98)
R^2	0.00	0.04	0.07	0.06	0.16
Memo: r^*		filtered	real-time	real-time	

Notes: Predictive regressions for annual average excess bond returns $\overline{rx}_{t+1} \equiv \frac{1}{14}\sum_{n=2}^{15} rx_{t+1}^{(n)}$. The independent variables are OLS residuals in the regressions for the trend variables on the observed 1- to 15-year yields. Numbers in parentheses are Newey-West standard errors.

Table 7: Contemporaneous responses of risk-neutral yields and term premia to monetary policy shocks.

	Daily Change				Window Change			
	TP5	RNY5	TP10	RNY10	TP5	RNY5	TP10	RNY10
MPS_ORTH	0.039***	0.481***	0.075**	0.559***	0.077***	0.570***	0.149***	0.577***
	(0.015)	(0.090)	(0.031)	(0.093)	(0.018)	(0.102)	(0.040)	(0.097)
Observations	281	281	281	281	281	281	281	281
R^2	0.041	0.188	0.032	0.239	0.089	0.150	0.071	0.158
Adjusted R^2	0.037	0.185	0.029	0.236	0.085	0.147	0.067	0.155
MPS	0.038***	0.508***	0.067**	0.563***	0.076***	0.640***	0.140***	0.619***
	(0.012)	(0.082)	(0.026)	(0.087)	(0.017)	(0.093)	(0.037)	(0.104)
Observations	281	281	281	281	281	281	281	281
R^2	0.046	0.257	0.031	0.298	0.106	0.233	0.076	0.223
Adjusted R^2	0.043	0.254	0.028	0.295	0.102	0.230	0.073	0.221

*p<0.1; **p<0.05; ***p<0.01

Notes: The term premia and risk-neutral yields are computed from the OSE: ∇y_t model. The regression is $\Delta^{FOMC} y_t^{(n),\cdot} = \beta_0 + \beta_1 HFS_t + \varepsilon_t$. The dependent variable $\Delta^{FOMC} y_t^{(n),\cdot}$ is the daily changes in the n-year term premium or term premium on the FOMC announcement dates or the $t-1$-to-$t+1$ changes around FOMC announcement dates. TP5 and RNY5 denote the 5-year term premium and risk-neutral yields, and those for the 10-year yield are denoted analogously. The high-frequency shock HFS_s is the 30-minute change in the policy rate futures rate bracketing the FOMC announcement time. The shock MPS is the first principal component of the changes in ED1-ED4, scaled so that the impact on ED4 is unity. The shock MPS_ORTH is the orthogonalized MPS computed by Bauer and Swanson (2022b).

Table 8: Model-implied predictive R^2 of excess bond returns.

	(1) R^2 PCs only	(2) R^2 with ∇y_t	(3) (2)-(1)
Data	0.23	0.52	0.29
FE model	0.31	0.35	0.05
	[0.18, 0.46]	[0.23, 0.51]	[0.00, 0.19]
OSE model	0.42	0.62	0.19
	[0.25, 0.60]	[0.47, 0.74]	[0.07, 0.34]
ESE model	0.41	0.55	0.14
	[0.22, 0.61]	[0.37, 0.72]	[0.03, 0.29]

Notes: The R^2 of predictive regressions for annual excess bond returns, averaged across maturities of 2 to 15 years. The R^2 in the data corresponds to the full-sample estimates in the main text. The model-implied R^2 are based on 5,000 simulations of artificial data of the same size as the full sample. For each model, the first row reports the means and the second row reports the 95 percent Monte Carlo confidence intervals of the R^2 of predictive regressions estimated in the simulated data.

Table 9: Predicting annual excess bond returns: inflation and output trends.

	(1)	(2)	(3)	(4)	(5)
Panel A: Full sample, 1989-2020					
PC1	0.84	6.23	7.51	7.65	12.33
	(0.55)	(1.55)	(1.72)	(1.58)	(2.02)
PC2	-0.01	-0.01	-0.01	-0.02	-0.01
	(0.00)	(0.00)	(0.00)	(0.00)	(0.00)
PC3	-3.53	-2.82	-2.56	-2.27	-1.77
	(1.49)	(1.35)	(1.30)	(1.13)	(1.30)
π_t^*		-14.10	-13.62	-10.07	
		(3.71)	(3.46)	(3.75)	
		[0.12]	[0.10]	[0.30]	
g_t^*			-5.62		
			(3.40)		
			[0.54]		
x_t^*				3.96	
				(1.13)	
				[0.12]	
∇y_t					-14.67
					(2.46)
					[0.01]
R^2	0.19	0.35	0.38	0.43	0.46
Memo: output trend			trend growth	output gap	
Panel B: Subsample, 1994-2020					
PC1	1.70	6.28	6.73	6.94	11.86
	(0.66)	(1.70)	(1.73)	(1.55)	(1.94)
PC2	-0.01	-0.01	-0.01	-0.02	-0.01
	(0.00)	(0.00)	(0.00)	(0.00)	(0.00)
PC3	-2.77	-2.28	-2.16	-1.51	-1.35
	(1.55)	(1.37)	(1.34)	(1.12)	(1.42)
π_t^*		-16.14	-13.01	-7.14	
		(5.44)	(6.53)	(5.01)	
		[0.33]	[0.47]	[0.73]	
g_t^*			-4.35		
			(4.52)		
			[0.77]		
x_t^*				4.51	
				(1.15)	
				[0.05]	
∇y_t					-14.33
					(2.63)
					[0.04]
R^2	0.21	0.31	0.33	0.40	0.44
Memo: output trend			trend growth	output gap	

Notes: Predictive regressions for annual average excess bond returns $\overline{rx}_{t+1} \equiv \frac{1}{14}\sum_{n=2}^{15} rx_{t+1}^{(n)}$. The independent variables are the first three principal components of yields (PC1, PC2, PC3), estimates of the inflation trend π_t^*, the real output growth trend g_t^*, the output gap x_t, and the first principal component of cumulative changes in yields during the FOMC window ∇y_t. The numbers in parentheses are Newey-West standard errors, and those in square brackets are small-sample p values à la Bauer and Hamilton (2018).

References

Adrian, T., R. K. Crump, and E. Moench (2013): "Pricing the term structure with linear regressions," *Journal of Financial Economics*, 110, 110–138, 10.1016/j.jfineco.2013.04.009.

Bauer, M. D., and J. D. Hamilton (2018): "Robust Bond Risk Premia," *The Review of Financial Studies*, 31, 399–448, 10.1093/rfs/hhx096.

Bauer, M. D., and G. D. Rudebusch (2017): "Resolving the Spanning Puzzle in Macro-Finance Term Structure Models*," *Review of Finance*, 21, 511–553, 10.1093/rof/rfw044.

——— (2020): "Interest Rates under Falling Stars," *American Economic Review*, 110, 1316–1354, 10.1257/aer.20171822.

Bauer, M. D., and E. T. Swanson (2022a): "An Alternative Explanation for the "Fed Information Effect"," April, 10.3386/w27013.

——— (2022b): "A Reassessment of Monetary Policy Surprises and High-Frequency Identification," in *NBER Macroeconomics Annual 2022, volume 37*: University of Chicago Press, `https://www.nber.org/books-and-chapters/nber-macroeconomics-annual-2022-volume-37/reassessment-monetary-policy-surprises-and-high-frequency-identification`.

Bernanke, B. (2005): "The global saving glut and the US current account deficit,"Technical report, Board of Governors of the Federal Reserve System (US).

Campbell, J. Y., and R. J. Shiller (1987): "Cointegration and tests of present value models," *Journal of political economy*, 95, 1062–1088.

——— (1991): "Yield Spreads and Interest Rate Movements: A Bird's Eye View," *The Review of Economic Studies*, 58, 495–514, 10.2307/2298008, Publisher: [Oxford University Press, Review of Economic Studies, Ltd.].

Carvalho, C., A. Ferrero, and F. Nechio (2016): "Demographics and real interest rates: Inspecting the mechanism," *European Economic Review*, 88, 208–226.

Cieslak, A., and P. Povala (2015): "Expected returns in Treasury bonds," *The Review of Financial Studies*, 28, 2859–2901.

Cochrane, J. H., and M. Piazzesi (2005): "Bond Risk Premia," *American Economic Review*, 95, 138–160, 10.1257/0002828053828581.

Del Negro, M., G. Eggertsson, A. Ferrero, and N. Kiyotaki (2017a): "The Great Escape? A Quantitative Evaluation of the Fed's Liquidity Facilities," *American Economic Review*, 107, 824–857, 10.1257/aer.20121660.

Del Negro, M., D. Giannone, M. P. Giannoni, and A. Tambalotti (2017b): "Safety, liquidity, and the natural rate of interest," *Brookings Papers on Economic Activity*, 2017, 235–316.

——— (2019): "Global trends in interest rates," *Journal of International Economics*, 118, 248–262, 10.1016/j.jinteco.2019.01.010.

Diebold, F. X., and R. S. Mariano (1995): "Comparing Predictive Accuracy," *Journal of Business & Economic Statistics*, 13, 253–263, 10.1198/073500102753410444, Publisher: Taylor & Francis _eprint: https://doi.org/10.1198/073500102753410444.

Drechsler, I., A. Savov, and P. Schnabl (2018): "A Model of Monetary Policy and Risk Premia," *The Journal of Finance*, 73, 317–373, 10.1111/jofi.12539.

Duffee, G. (2013): "Chapter 7 - Forecasting Interest Rates," in *Handbook of Economic Forecasting* ed. by Elliott, G., and Timmermann, A. Volume 2 of Handbook of Economic Forecasting: Elsevier, 385–426, 10.1016/B978-0-444-53683-9.00007-4.

Eichengreen, B. (2015): "Secular stagnation: the long view," *American Economic Review*, 105, 66–70.

Fama, E. F., and R. R. Bliss (1987): "The Information in Long-Maturity Forward Rates," *The American Economic Review*, 77, 680–692, https://www.jstor.org/stable/1814539, Publisher: American Economic Association.

Gagnon, E., B. K. Johannsen, and D. Lopez-Salido (2021): "Understanding the new normal: The role of demographics," *IMF Economic Review*, 69, 357–390.

Gertler, M., and P. Karadi (2015): "Monetary Policy Surprises, Credit Costs, and Economic Activity," *American Economic Journal: Macroeconomics*, 7, 44–76, 10.1257/mac.20130329.

Gordon, R. (2017): *The rise and fall of American growth: The US standard of living since the civil war*: Princeton University Press.

Gürkaynak, R. S., B. Sack, and J. H. Wright (2007): "The US Treasury yield curve: 1961 to the present," *Journal of monetary Economics*, 54, 2291–2304.

Gürkaynak, R. S., B. Sack, and E. Swanson (2005a): "The Sensitivity of Long-Term Interest Rates to Economic News: Evidence and Implications for Macroeconomic Models," *American Economic Review*, 95, 425–436, 10.1257/0002828053828446.

——— (2005b): "Do Actions Speak Louder Than Words? The Response of Asset Prices to Monetary Policy Actions and Statements," *International Journal of Central Banking*, https://www.ijcb.org/journal/ijcb05q2a2.htm.

Gürkaynak, R. S., B. Sack, and J. H. Wright (2007): "The U.S. Treasury yield curve: 1961 to the present," *Journal of Monetary Economics*, 54, 2291–2304, 10.1016/j.jmoneco.2007.06.029.

Gürkaynak, R. S., and J. H. Wright (2012): "Macroeconomics and the Term Structure," *Journal of Economic Literature*, 50, 331–367, 10.1257/jel.50.2.331.

Hall, A. D., H. M. Anderson, and C. W. Granger (1992): "A cointegration analysis of treasury bill yields," *The review of Economics and Statistics*, 116–126.

Hanson, S. G., and J. C. Stein (2015): "Monetary policy and long-term real rates," *Journal of Financial Economics*, 115, 429–448, 10.1016/j.jfineco.2014.11.001.

Harvey, A. C. (1989): "Forecasting, Structural Time Series Models and the Kalman Filter."

Hillenbrand, S. (2021): "The Fed and the secular decline in interest rates," *Available at SSRN 3550593*.

Holston, K., T. Laubach, and J. C. Williams (2017): "Measuring the natural rate of interest: International trends and determinants," *Journal of International Economics*, 108, S59–S75.

Jarociński, M., and P. Karadi (2020): "Deconstructing Monetary Policy Surprises— The Role of Information Shocks," *American Economic Journal: Macroeconomics*, 12, 1–43, 10.1257/mac.20180090.

Johannsen, B. K., and E. Mertens (2016): "The Expected Real Interest Rate in the Long Run: Time Series Evidence with the Effective Lower Bound,"Technical report, Board of Governors of the Federal Reserve System (US).

Joslin, S., M. Priebsch, and K. J. Singleton (2014): "Risk Premiums in Dynamic Term Structure Models with Unspanned Macro Risks," *The Journal of Finance*, 69, 1197–1233, 10.1111/jofi.12131, _eprint: https://onlinelibrary.wiley.com/doi/pdf/10.1111/jofi.12131.

Joslin, S., K. J. Singleton, and H. Zhu (2011): "A new perspective on Gaussian dynamic term structure models," *The Review of Financial Studies*, 24, 926–970.

Kekre, R., and M. Lenel (2022): "Monetary Policy, Redistribution, and Risk Premia," *Econometrica*, 90, 2249–2282, 10.3982/ECTA18014, _eprint: https://onlinelibrary.wiley.com/doi/pdf/10.3982/ECTA18014.

Kiley, M. T. (2020): "What Can the Data Tell Us about the Equilibrium Real Interest Rate?" *International Journal of Central Banking*, 16, 181–209.

Kim, D. H., and J. H. Wright (2005): "An arbitrage-free three-factor term structure model and the recent behavior of long-term yields and distant-horizon forward rates."

Kozicki, S., and P. A. Tinsley (2001): "Shifting endpoints in the term structure of interest rates," *Journal of monetary Economics*, 47, 613–652.

Kuttner, K. N. (2001): "Monetary policy surprises and interest rates: Evidence from the Fed funds futures market," *Journal of Monetary Economics*, 47, 523–544, 10.1016/S0304-3932(01)00055-1.

Lagos, R., and S. Zhang (2020): "Turnover Liquidity and the Transmission of Monetary Policy," *American Economic Review*, 110, 1635–1672, 10.1257/aer.20170045.

Laubach, T., and J. C. Williams (2003): "Measuring the Natural Rate of Interest," *The Review of Economics and Statistics*, 85, 1063–1070, `https://www.jstor.org/stable/3211826`, Publisher: The MIT Press.

——— (2016): "Measuring the natural rate of interest redux," *Business Economics*, 51, 57–67.

Ludvigson, S. C., and S. Ng (2009): "Macro Factors in Bond Risk Premia," *The Review of Financial Studies*, 22, 5027–5067, 10.1093/rfs/hhp081.

Müller, U. K., and M. W. Watson (2013): "Low-frequency robust cointegration testing," *Journal of Econometrics*, 174, 66–81, 10.1016/j.jeconom.2012.09.006.

Pflueger, C., and G. Rinaldi (2022): "Why does the Fed move markets so much? A model of monetary policy and time-varying risk aversion," *Journal of Financial Economics*, 146, 71–89, 10.1016/j.jfineco.2022.06.002.

Piazzesi, M. (2005): "Bond Yields and the Federal Reserve," *Journal of Political Economy*, 113, 311–344, 10.1086/427466, Publisher: The University of Chicago Press.

Stock, J. H., and M. W. Watson (1993): "A Simple Estimator of Cointegrating Vectors in Higher Order Integrated Systems," *Econometrica*, 61, 783–820, 10.2307/2951763, Publisher: [Wiley, Econometric Society].

Summers, L. H. (2014): "Reflections on the 'new secular stagnation hypothesis'," *Secular stagnation: Facts, causes and cures*, 1, 27–40.

Svensson, L. E. (1994): "Estimating and Interpreting Forward Interest Rates: Sweden 1992 - 1994," September, 10.3386/w4871.

Wright, J. H. (2011): "Term Premia and Inflation Uncertainty: Empirical Evidence from an International Panel Dataset," *American Economic Review*, 101, 1514–1534, 10.1257/aer.101.4.1514.

——— (2012): "What does Monetary Policy do to Long-term Interest Rates at the Zero Lower Bound?" *The Economic Journal*, 122, F447–F466, 10.1111/j.1468-0297.2012.02556.x.

A Model

The model is proposed by Bauer and Rudebusch (2020). We propose a new estimation method that avoids numerical optimization and speeds up the estimation. The estimation method allows for vector-valued trends for the state vector, and the scalar-τ_t model is a special case.

A.1 Model Setup

The state is a $K_X \times 1$ vector X_t, which evolves as

$$
\begin{aligned}
X_t =& \boldsymbol{\mu} + \Gamma \boldsymbol{\tau}_t + \tilde{X}_t, \\
\boldsymbol{\tau}_t =& \boldsymbol{\tau}_{t-1} + \boldsymbol{\eta}_t, \quad \boldsymbol{\eta}_t \sim \mathcal{N}(0, \Omega_\eta) \\
\tilde{X}_t =& \Phi \tilde{X}_{t-1} + \tilde{U}_t, \quad \tilde{U}_t \sim \mathcal{N}(0, \tilde{\Omega}),
\end{aligned}
\tag{A1}
$$

where $\boldsymbol{\tau}_t$ is a $K_\tau \times 1$ random walk and $\tilde{X}_t$ is a $K_X \times 1$ stationary VAR(1). The shocks are i.i.d over time and $\boldsymbol{\eta}_t \perp \tilde{U}_t$. Define

$$
Z_t \equiv \begin{bmatrix} \boldsymbol{\tau}_t \\ X_t \end{bmatrix}, U_t \equiv \Gamma \boldsymbol{\eta}_t + \tilde{U}_t, \Omega \equiv \mathbf{E}[U_t U_t^\top] = \Gamma \Omega_\eta \Gamma^\top + \tilde{\Omega}.
$$

The log stochastic discount factor m_{t+1} evolves as

$$
m_{t+1} = -\delta_0 - \boldsymbol{\delta}_1^\top X_t - \frac{1}{2} \Lambda_t^\top \Lambda_t - \Lambda_t^\top \Omega^{-\frac{1}{2}} U_{t+1}. \tag{A2}
$$

The price of risk is an affine function of Z_t:

$$
\Lambda_t = \Omega^{-\frac{1}{2}} (\Lambda_0 + \Lambda_1 Z_t). \tag{A3}
$$

Note that the SDF is driven by a $K_X \times 1$ dimensional shock with the same dimension as X_t, but is a combination of shocks to $\boldsymbol{\tau}_t$ and $\tilde{X}_t$. Although the trend $\boldsymbol{\tau}_t$ does not directly affect the observed yields, it affects risk premia by affecting the price of risk. We assume that Λ_1 satisfies

$$
\Lambda_1 = \left[(I_{K_X} - \Phi)\Gamma, \Lambda_{12} \right], \tag{A4}
$$

i.e., the first K_τ column of Λ_1 (the loading on $\boldsymbol{\tau}_t$) equals $(I_{K_X} - \Phi)\Gamma$ and the remaining K columns is an unrestricted $K_X \times K$ matrix Λ_{12}. It can be shown that the log zero-coupon bond prices are affine in X_t:

$$
p_t^{(n)} = \mathcal{A}_n + \mathcal{B}_n^\top X_t, \tag{A5}
$$

where $\mathcal{A}_n$ and $\mathcal{B}_n$ satisfy the usual no-arbitrage recursions.

A.2 No-Arbitrage Recursions

First, we show that the state vector Z_t evolves as

$$Z_t = \boldsymbol{\mu}_Z + \Phi_Z Z_{t-1} + V_t, \quad V_t \equiv \begin{bmatrix} \boldsymbol{\eta}_t \\ U_t \end{bmatrix}, \tag{A6}$$

with

$$\boldsymbol{\mu}_Z = \begin{bmatrix} 0 \\ (I_{K_X} - \Phi)\boldsymbol{\mu} \end{bmatrix}, \quad \Phi_Z = \begin{bmatrix} I_{K_\tau} & 0_{K_\tau \times K_X} \\ (I_{K_X} - \Phi)\Gamma & \Phi \end{bmatrix}, \quad \Omega_V \equiv \mathbf{E}[V_t V_t^\top] = \begin{bmatrix} \Omega_\eta & \Omega_\eta \Gamma^\top \\ \Gamma\Omega_\eta & \Omega \end{bmatrix}.$$

We rewrite Z_t as

$$Z_t = \begin{bmatrix} 0 \\ \boldsymbol{\mu} \end{bmatrix} + \begin{bmatrix} I_{K_\tau} & 0_{K_\tau \times K_X} \\ \Gamma & \Phi \end{bmatrix} \begin{bmatrix} \boldsymbol{\tau}_{t-1} \\ \tilde{X}_{t-1} \end{bmatrix} + \begin{bmatrix} \boldsymbol{\eta}_t \\ \Gamma \boldsymbol{\eta}_t + \tilde{U}_t. \end{bmatrix}$$

Note that

$$\begin{bmatrix} \boldsymbol{\tau}_{t-1} \\ \tilde{X}_{t-1} \end{bmatrix} = \begin{bmatrix} 1 & 0_{K_\tau \times K_X} \\ -\Gamma & I_{K_X} \end{bmatrix} \begin{bmatrix} \boldsymbol{\tau}_{t-1} \\ X_{t-1} \end{bmatrix} - \begin{bmatrix} 0 \\ \boldsymbol{\mu} \end{bmatrix}.$$

Substituting for $\boldsymbol{\tau}_{t-1}$ and $\tilde{X}_{t-1}$, we get $\boldsymbol{\mu}_Z, \phi_Z$ and V_t. Since $V_t \perp \tilde{U}_t$, the expression for Ω_V follows naturally.

Next, we show that restriction (A4) implies the bond pricing equation (A5). We prove by guess-and-verify. The no-arbitrage recursion is

$$p_t^{(n)} = \mathbf{E}_t[m_{t+1}] + \mathbf{E}_t[p_{t+1}^{(n-1)}] + \frac{1}{2}\mathbf{Var}_t(m_{t+1}) + \frac{1}{2}\mathbf{Var}_t(p_{t+1}^{(n-1)}) + \mathbf{Cov}_t(m_{t+1}, p_{t+1}^{(n-1)}). \tag{A7}$$

Note that $\mathbf{E}_t[\cdot]$ refers $\mathbf{E}[\cdot|Z_t]$, and

$$\begin{aligned} \mathbf{E}_t[X_{t+1}] =& \boldsymbol{\mu} + \Gamma\boldsymbol{\tau}_t + \Phi\tilde{X}_t = \boldsymbol{\mu} + \Gamma\boldsymbol{\tau}_t + \Phi(X_t - \boldsymbol{\mu} - \Gamma\boldsymbol{\tau}_t) \\ =& (I_{K_X} - \Phi)(\boldsymbol{\mu} + \Gamma\boldsymbol{\tau}_t) + \Phi X_t. \end{aligned}$$

When $p_t^{(n)} = \mathcal{A}_n + \mathcal{B}_n^\top X_t$,

$$\mathbf{E}_t[m_{t+1}] + \frac{1}{2}\mathbf{Var}_t(m_{t+1}) = -\delta_0 - \boldsymbol{\delta}_1^\top X_t,$$

$$\mathbf{E}_t[p_{t+1}^{(n-1)}] = \mathcal{A}_{n-1} + \mathcal{B}_{n-1}^\top[(I_{K_X} - \Phi)(\boldsymbol{\mu} + \Gamma\boldsymbol{\tau}_t) + \Phi X_t],$$

$$\mathbf{Var}_t(p_{t+1}^{(n-1)}) = \mathcal{B}_{n-1}^\top \Omega \mathcal{B}_{n-1},$$

$$\mathbf{Cov}_t(m_{t+1}, p_{t+1}^{(n-1)}) = -\mathcal{B}_{n-1}^\top (\Lambda_0 + \Lambda_1 Z_t).$$

Note that $\Lambda_1 Z_t = \Lambda_{11}\boldsymbol{\tau}_t + \Lambda_{12} X_t$, and we hope to eliminate $\boldsymbol{\tau}_t$ from the right-hand side of the recursion. Collecting the terms involving $\boldsymbol{\tau}_t$, we should have

$$\mathcal{B}_{n-1}^\top [(I_{K_X} - \Phi)\Gamma - \Lambda_{11}] = 0, \quad \forall n.$$

So $\Lambda_{11} = (I_{K_X} - \Phi)\Gamma$ eliminates $\boldsymbol{\tau}_t$ from the right-hand side of Equation (A7).

Finally, we derive the bond pricing recursions. Equation (A7) together with Equation (A4) implies

$$p_t^{(n)} = -\delta_0 - \boldsymbol{\delta}_1^\top X_t + \mathcal{A}_{n-1} + \mathcal{B}_{n-1}^\top [(I_{K_X} - \Phi)\boldsymbol{\mu} + \Phi X_t] \tag{A8}$$

$$+ \frac{1}{2}\mathcal{B}_{n-1}^\top \Omega \mathcal{B}_{n-1} - \mathcal{B}_{n-1}^\top (\Lambda_0 + \Lambda_{12} X_t). \tag{A9}$$

So,

$$\mathcal{A}_n = \mathcal{A}_{n-1} - \delta_0 + \mathcal{B}_{n-1}^\top (I_{K_X} - \Phi)\boldsymbol{\mu} + \frac{1}{2}\mathcal{B}_{n-1}^\top \Omega \mathcal{B}_{n-1} - \mathcal{B}_{n-1}^\top \Lambda_0, \tag{A10}$$

$$\mathcal{B}_n^\top = -\boldsymbol{\delta}_1^\top + \mathcal{B}_{n-1}^\top (\Phi - \Lambda_{12}). \tag{A11}$$

The yields are

$$y_t^{(n)} = A_n + B_t^\top X_t, \tag{A12}$$

with $A_n = -\frac{1}{n}\mathcal{A}_n$ and $B_n = -\frac{1}{n}\mathcal{B}_n$.

B Estimation

[To be written]

C Additional Results

C.1 Cointegration Test for the Average Yield

We estimate cointegration relationships between the first principal component of 3-month, 6-month, and 1-year through 15-year Treasury yields. Details are described in Section 2, and the regressions are the same as those in Table 2. The sample period is 1990Q1-2018Q1. The results are qualitatively similar to those reported in Table 2 for the 10-year yield.

Quantitatively, the cointegration residuals are more persistent than those for the 10-year yield. The only residuals that significantly reject the unit root hypothesis regarding ADF and PP tests are the demeaned average[9] cumulative changes in yields outside FOMC windows and residuals obtained by regressing on ∇y_t.

Table A1 about here.

C.2 Predicting Excess Bond Returns

In the paper, we study excess bond returns over the holding period of one year. In Table A2, we report the predictive regression results analogous to those reported in Table 3, but over the holding period of one quarter. The regression R^2s for the quarterly holding period are smaller than those for the annual holding period. However, we focus on (i) the improvement in R^2 by including trend variables, and (ii) the significance of the trend variables. For the quarterly holding period, we also find that (i) ∇y_t leads to the largest improvement in R^2, and (ii) ∇y_t is highly significant. The results are consistent with those reported in Table 3.

Table A2 about here.

Monetary policy reacts to macroeconomic conditions. For example, the standard Taylor rule stipulates that the policy interest rate is a linear combination of inflation and the output gap, plus an unexpected "monetary policy shock". Therefore, the monetary policy trend ∇y_t may be equivalent to a linear combination of the inflation and output growth/gap trends. In this case, our main argument that the secular trend in Treasury yields is driven by the monetary policy trend is equivalent to the classical inflation-driven or output-driven mechanisms for the interest rate trend. To rule out this possibility, we test whether a linear combination of the inflation and output trends has a similar predictive performance as ∇y_t. We run the regression

$$\overline{rx}_{t+1} = \alpha + \boldsymbol{PC}_t^\top \boldsymbol{\beta} + \boldsymbol{\tau}_t^\top \boldsymbol{\gamma} + \varepsilon_{t+1}, \tag{A13}$$

where $\boldsymbol{\tau}_t$ is a vector of the inflation trend and output factor. For the output factor, we consider the real output growth trend or the output gap estimated by Laubach and Williams (2003). Table A3 and Table 9 report regression results for the quarterly and annual holding periods. In both tables, ∇y_t provides the largest improvement in R^2 and is highly significant. The output factors are not significant for predicting excess bond returns. Therefore, ∇y_t is not equivalent to a linear combination of inflation and output factors. Monetary policy has

[9] Precisely, the first principal component of changes in all yields outside FOMC windows.

unique roles in determining the secular trend in Treasury yields, which is consistent with the similarity between the cumulative sums of (unexpected) monetary policy shocks and ∇y_t presented in Figure 4.

Table A3 about here.

Table 9 about here.

C.3 Using i_t^* as a Proxy for $\boldsymbol{\tau}_t$

Another proxy for $\boldsymbol{\tau}_t$ is the long-run nominal interest rate i_t^* in Bauer and Rudebusch (2020), which equals the sum of trend inflation and natural real interest rate. We compare the model-implied $y_t^{(10)*}$ using i_t^* or ∇y_t as a proxy for $\boldsymbol{\tau}_t$ in the OSE model. Since i_t* is quarterly, we also estimate the OSE: ∇y_t model at the quarterly frequency using end-of-quarter observations. Figure A1 presents the observed quarterly 10-year yield series along with its estimated trends. The trend series estimated by the ESE and i_t^* replicate Figure 5 of Bauer and Rudebusch (2020), and the $y_t^{(10)*}$ estimated from ∇y_t is also presented. The three estimates of $y_t^{(10)*}$ are very similar, confirming that the cumulative effects of monetary policy are essential for explaining the long-term trend of Treasury yields.

Figure A1 about here.

C.4 Yield Curve Decomposition: Shifting vs. Fixed Endpoints

How important is the shifting endpoint for understanding the effects of monetary policy on risk-neutral yields and term premia? We estimate risk-neutral yields and term premia components using the OSE: ∇y_t and the FE model and filter out their cumulative changes during or outside the FOMC windows. Figure A2 presents the filtered series for the two models. The thick solid curves are produced by the OSE model and the thin dotted curves are produced by the FE model. Since the FE model does not have a downward trend in the state variables, expected future short-term yields must revert to the unconditional mean as the horizon increases. Therefore, the risk-neutral yields implied by the FE model fail to incorporate the secular decline in the short-term interest rate. This is also reflected in the cumulative changes during the FOMC windows, especially for long maturities. For example, the OSE model suggests that the risk-neutral 10-year yield has declined by 5.2 percentage points during the FOMC windows since 1990, while the FE model suggests that it has declined by 3.6 percentage points. The FE model underestimates the effects of monetary policy on risk-neutral 10-year yields by 31%. Since the risk-neutral yield and term premium add up to the observed yield, the FE model overestimates the effects of monetary policy on term premia. The OSE model suggests that the 10-year term premium has declined by 2.5 percentage points during FOMC windows, and the FE model suggests that it has declined by 3.7 percentage points. Note that the FE model finds roughly equal effects of monetary policy on risk-neutral yields and term premia, which is also documented by Pflueger and Rinaldi (2022), who decompose the yields using a stationary DSGE model.

Figure A2 about here.

C.5 Out-of-Sample Forecasts

We use the OSE models to forecast out-of-sample Treasury yields and compare the performance with a random walk model. The random walk model has proven to be very hard to beat due to the extreme persistence of interest rates. Our results suggest that using ∇y_t as a proxy for $\boldsymbol{\tau}_t$ in a shifting-endpoint dynamic term structure model helps to achieve more accurate forecasts.

We compare the out-of-sample forecast performances of two proxies for $\boldsymbol{\tau}_t$: ∇y_t and the cumulative sums of daily changes in the federal funds target rate on FOMC announcement dates. The benchmark is a random walk with no drift, which uses the current value to forecast future values. The models are recursively estimated using monthly data, starting in January 1998 when five years of data are available[10]. We focus on forecasts of the 10-year yield at horizons of 1, 3, 12, 24, and 36 months. The root mean squared errors in annual percentage points are reported in Table A4. The table also reports p-values for the null hypothesis that two forecast models are equally accurate against the one-sided alternative that the left model is more accurate than the right model. The p-values are obtained by comparing the Diebold and Mariano (1995) statistic with standard normal critical values. We find that the OSE: ∇y_t is more accurate than the diftless random walk model at long forecast horizons, while the OSE: FF target model is outperformed by a random walk at all horizons.

Table A4 about here.

C.6 Monetary Policy Shocks and Yield Curve Decomposition

In the main text, we analyzed the effects of monetary policy shocks on risk-neutral yields and term premia. The monetary policy shocks in the main text are the first principal component of high-frequency ED1-ED4 shocks and its orthogonalized residual relative to

[10]Our sample starts from January 1994, when the federal funds target rate becomes available.

a set of macroeconomic news. Here, we present the effects of ED1-ED4 shocks on risk-neutral yields and term premia. We regress the three-day changes in the risk-neutral yields or term premia around FOMC announcements on each of the high-frequency futures shocks. Table A5 reports the estimation results. The results are consistent across all specifications: risk-neutral yields respond much more strongly to monetary policy shocks than term premia.

Table A5 about here.

Figure A1: Observed 10-year yield and its model-implied trend.

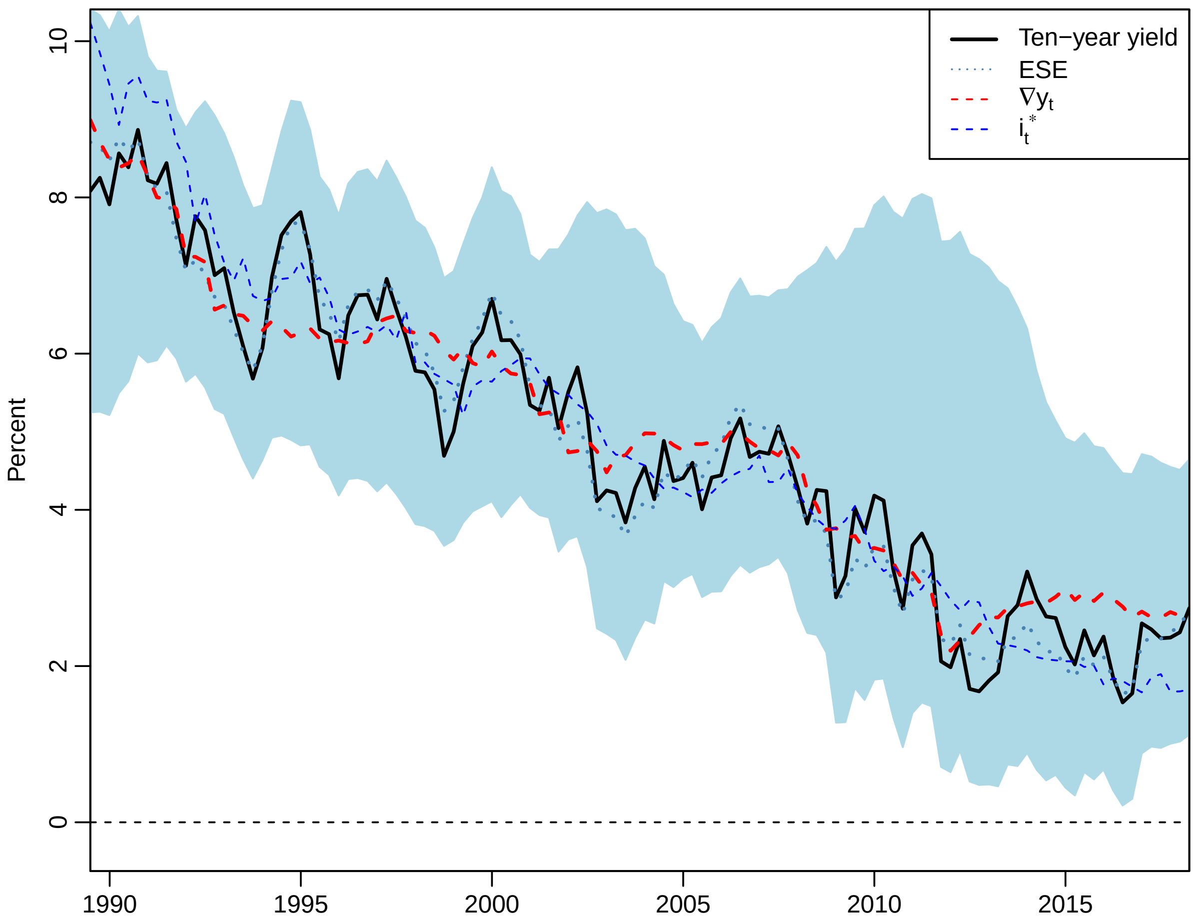

Notes: This figure estimates the trend component of the 10-year yield using either the OSE or the ESE approach. The solid curve is the observed 10-year Treasury yield. The trend is $y_t^{(10)*} = A_{10} + B_{10}(\mu + \Gamma\tau_t)$ using the model parameters A, B and the empirical proxy for τ_t. The red dashed curve is estimated from the OSE model using ∇y_t to proxy τ_t. The blue dashed curve is estimated from OSE model using the Bauer and Rudebusch (2020) trend nominal interest rate i_t^* to proxy τ_t. The dotted line is estimated from the Bauer and Rudebusch (2020) ESE model. The shaded area is the 95% Monte Carlo interval computed by Bauer and Rudebusch (2020).

Figure A2: Comparing yield curve decompositions based on the FE and OSE models.

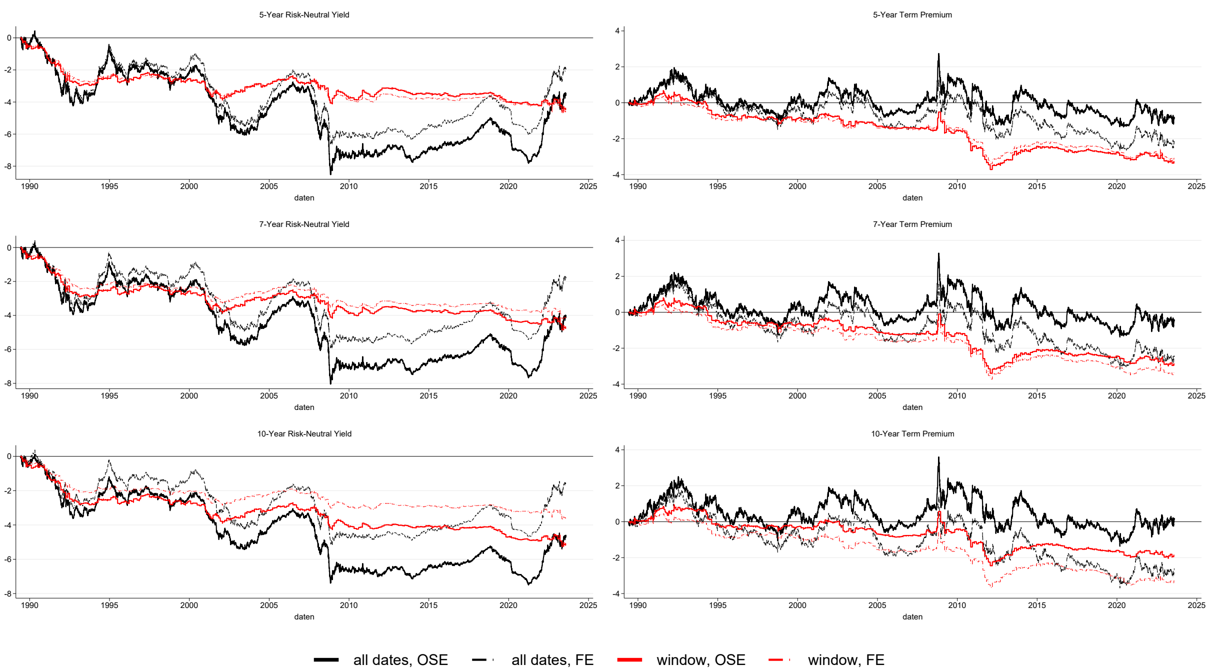

Notes: The FE model is the original model in Adrian et al. (2013), and the OSE model uses ∇y_t as the observed proxy fo τ_t. The black series are cumulative changes relative to the initial value using all daily observations, and the red series only sum over daily changes during FOMC windows.

Table A1: Cointegration tests for average yields and macroeconomic trends.

	$\bar{y}_t$	$\nabla y_t^{non-FOMC}$	(1)	(2)	(3)	(4)	(5)	(6)
constant	4.12	8.17	-0.90	-1.45	-3.64	-1.49	-4.34	-2.20
	(0.48)	(0.19)	(1.85)	(0.59)	(0.47)	(0.33)	(0.36)	(0.29)
π_t^*			1.99	1.31	1.97	1.73		
			(0.78)	(0.28)	(0.22)	(0.15)		
r_t^*				1.37	2.08	1.22		
				(0.16)	(0.10)	(0.07)		
i_t^*							2.21	
							(0.10)	
∇y_t								1.36
								(0.08)
R^2			0.44	0.88	0.96	0.97	0.94	0.90
Memo: r^*				filtered	real-time	mov. avg.	real-time	
SD	2.03	0.90	1.47	0.75	0.73	0.92	0.79	0.62
$\hat{\rho}$	0.95	0.86	0.94	0.82	0.78	0.86	0.80	0.76
Half-life	14.3	4.7	10.9	3.5	2.7	4.4	3.1	2.5
ADF	-1.85	-2.88*	-1.62	-3.26	-2.13	-2.11	-2.01	-3.67*
PP	-4.76	-14.82**	-6.64	-21.06	-14.50	-9.66	-11.39	-27.23**
LFST	0.00	0.00	0.01	0.50	0.70	0.34	0.35	0.60
Johansen $r=0$			25.20***	42.75***	58.56***	63.63***	36.94***	23.19**
Johansen $r=1$			3.37	16.40	22.15**	26.76***	7.41	8.37*
ECM $\hat{\alpha}$			-0.06	-0.16	-0.23	-0.49	-0.14	-0.26
			(0.03)	(0.07)	(0.10)	(0.17)	(0.09)	(0.08)

Notes: * $p < 0.1$, ** $p < 0.05$, *** $p < 0.01$. Dynamic OLS regressions of the first principal component of the yield curve on macroeconomic trends, including four leads and lags of the yield and differenced trend variables. Newey-West standard errors with 6 lags are in parentheses. The estimates of $\pi_t t^*$ and r_t^* are from Bauer and Rudebusch (2020) and i_t^* is the sum of π_t^* and the real-time r_t^*. ∇y_t is the first principal component of cumulative changes in all Treasury yields during FOMC windows. The second panel reports statistics for the cointegration residuals, including standard deviations (SD), first-order autocorrelation coefficients ($\hat{\rho}$), half-lives ($\ln(0.5)/\ln(\hat{\rho})$), Augmented Dickey-Fuller (ADF) and Phillips-Perron (PP) unit root test statistics, and p-values for Müller-Watson low-frequency stationary test (LFST). The third panel reports statistics for an error-correction model for first differences of the yield and each macroeconomic trend. The model includes four lags and a constant. The statistics reported are the Johansen trace statistic for the cointegration rank (r) between the yield and macroceconomic trend against the alternative that the rank exceeds the specified level, and the loading of the differenced yield on the cointegrated variable (ECM $\hat{\alpha}$).

Table A2: Predicting quarterly excess bond returns.

	(1)	(2)	(3)	(4)	(5)	(6)	(7)
			Panel A: Full sample, 1989-2018				
PC1	0.21	0.51	1.37	2.38	2.12	2.49	2.67
	(0.12)	(0.20)	(0.34)	(0.58)	(0.51)	(0.47)	(0.52)
PC2	0.31	0.40	0.47	0.61	0.60	0.52	0.58
	(0.12)	(0.11)	(0.10)	(0.13)	(0.13)	(0.12)	(0.13)
PC3	-1.42	-1.30	-0.56	0.75	0.38	-0.15	0.18
	(0.89)	(0.89)	(1.01)	(1.20)	(1.03)	(1.03)	(1.03)
π_t^*		-1.43	-2.48	-4.02			
		(0.63)	(0.68)	(0.96)			
		[0.19]	[0.04]	[0.02]			
r_t^*			-1.53	-5.06			
			(0.61)	(1.59)			
			[0.11]	[0.10]			
i_t^*					-4.03		-1.25
					(0.99)		(1.17)
					[0.02]		[0.45]
∇y_t						-3.27	-2.68
						(0.63)	(0.80)
						[0.00]	[0.02]
R^2	0.07	0.09	0.12	0.15	0.15	0.18	0.18
Memo: r^*			filtered	real-time	real-time		real-time
			Panel B: Subsample, 1994-2018				
PC1	0.31	0.50	1.58	2.26	2.28	2.53	3.00
	(0.16)	(0.25)	(0.50)	(0.66)	(0.66)	(0.53)	(0.70)
PC2	0.33	0.39	0.49	0.60	0.59	0.48	0.57
	(0.15)	(0.13)	(0.11)	(0.16)	(0.16)	(0.16)	(0.17)
PC3	-1.21	-1.36	-0.66	0.50	0.56	-0.14	0.46
	(0.94)	(0.92)	(0.97)	(1.24)	(1.13)	(1.04)	(1.16)
π_t^*		-1.94	-4.54	-4.92			
		(1.81)	(2.21)	(2.22)			
		[0.52]	[0.25]	[0.25]			
r_t^*			-1.77	-4.63			
			(0.70)	(1.65)			
			[0.12]	[0.25]			
i_t^*					-4.73		-2.18
					(1.55)		(1.49)
					[0.16]		[0.34]
∇y_t						-3.53	-2.83
						(0.87)	(0.85)
						[0.03]	[0.03]
R^2	0.07	0.08	0.12	0.14	0.14	0.18	0.19
Memo: r^*			filtered	real-time	real-time		real-time

Notes: Predictive regressions for quarterly average excess bond returns $\overline{rx}_{t+1} \equiv \frac{1}{14}\sum_{n=2}^{15} rx_{t+1}^{(n)}$. The independent variables are the first three principal components of yields (PC1, PC2, PC3), estimates of the inflation trend π_t^*, the real-rate trend r_t^*, and the long-run nominal short rate i_t^*, and the first principal component of cumulative changes in yields during the FOMC window ∇y_t. The numbers in parentheses are Newey-West standard errors and in square brackets are small-sample p values obtained with the bootstrap method of Bauer and Hamilton (2018).

Table A3: Predicting quarterly excess bond returns: inflation and output trends.

	(1)	(2)	(3)	(4)	(5)
			Panel A: Full sample, 1989-2020		
PC1	0.25	2.00	2.40	2.61	5.09
	(0.24)	(0.76)	(0.90)	(0.79)	(1.10)
PC2	-0.00	-0.00	-0.00	-0.01	-0.00
	(0.00)	(0.00)	(0.00)	(0.00)	(0.00)
PC3	-1.11	-0.87	-0.78	-0.63	-0.39
	(0.53)	(0.57)	(0.58)	(0.63)	(0.61)
π_t^*		-4.69	-4.50	-2.99	
		(1.68)	(1.67)	(1.69)	
		[0.15]	[0.14]	[0.39]	
g_t^*			-1.84		
			(1.56)		
			[0.58]		
x_t^*				1.68	
				(0.71)	
				[0.19]	
∇y_t					-6.14
					(1.30)
					[0.01]
R^2	0.04	0.09	0.10	0.12	0.17
Memo: output trend			trend growth	output gap	
			Panel B: Subsample, 1994-2020		
PC1	0.45	2.31	2.42	2.60	5.17
	(0.33)	(0.95)	(1.02)	(0.88)	(1.18)
PC2	-0.00	-0.00	-0.00	-0.01	-0.00
	(0.00)	(0.00)	(0.00)	(0.00)	(0.00)
PC3	-0.91	-0.70	-0.67	-0.41	-0.30
	(0.58)	(0.56)	(0.57)	(0.64)	(0.64)
π_t^*		-6.72	-5.93	-3.34	
		(2.92)	(3.14)	(3.23)	
		[0.33]	[0.36]	[0.75]	
g_t^*			-1.09		
			(2.06)		
			[0.84]		
x_t^*				1.73	
				(0.78)	
				[0.15]	
∇y_t					-6.53
					(1.58)
					[0.03]
R^2	0.03	0.08	0.08	0.11	0.16
Memo: output trend			trend growth	output gap	

Notes: Predictive regressions for quarterly average excess bond returns $\overline{rx}_{t+1} \equiv \frac{1}{14}\sum_{n=2}^{15} rx_{t+1}^{(n)}$. The independent variables are the first three principal components of yields (PC1, PC2, PC3), estimates of the inflation trend π_t^*, the real output growth trend g_t^*, the output gap x_t, and the first principal component of cumulative changes in yields during the FOMC window ∇y_t. The numbers in parentheses are Newey-West standard errors, and those in square brackets are small-sample p values obtained with the bootstrap method of Bauer and Hamilton (2018).

Table A4: Out-of-sample forecasts of the 10-year yield.

	1-mo	3-mo	12-mo	24-mo	36-mo
OSE: ∇y_t	0.28	0.44	0.62	0.73	0.97
OSE: FF target	0.29	0.49	0.89	1.23	1.45
Random walk	0.26	0.43	0.77	1.02	1.20
p-value: $\nabla y_t \succ$ FFR	0.01	0.03	0.02	0.02	0.04
p-value: $\nabla y_t \succ$ Random walk	0.98	0.74	0.01	0.02	0.03
p-value: FFR $\succ$ Random walk	1.00	0.99	0.92	0.95	0.93

Notes: The table reports root mean squared forecast errors of the 10-year yield in annual percentage points. The first row forecasts the yields with the OSE method, using ∇y_t as the proxy for τ_t. The second row uses the FOMC-window changes in the federal funds target rate as the proxy for τ_t. The third row forecasts the yields using a driftless random walk, i.e., the current value of the yields. The p-values are for testing the null hypothesis that the two forecast models are equally accurate against the one-sided alternative that the left model is more accurate than the right model. The test compares the Diebold and Mariano (1995) statistic with standard normal critical values.

Table A5: Contemporaneous responses of risk-neutral yields and term premia to monetary policy shocks.

	Daily Change				Window Change			
	TP5	RNY5	TP10	RNY10	TP5	RNY5	TP10	RNY10
ED1	0.035***	0.398***	0.058***	0.377**	0.064***	0.587***	0.110***	0.492***
	(0.010)	(0.126)	(0.021)	(0.154)	(0.018)	(0.142)	(0.039)	(0.161)
Observations	282	282	282	282	282	282	282	282
R^2	0.044	0.177	0.027	0.149	0.084	0.219	0.052	0.159
Adjusted R^2	0.041	0.174	0.023	0.146	0.081	0.216	0.049	0.156
ED2	0.036***	0.431***	0.063***	0.438***	0.068***	0.590***	0.119***	0.532***
	(0.010)	(0.105)	(0.022)	(0.134)	(0.016)	(0.109)	(0.035)	(0.133)
Observations	282	282	282	282	282	282	282	282
R^2	0.049	0.214	0.032	0.207	0.095	0.228	0.064	0.191
Adjusted R^2	0.046	0.211	0.029	0.204	0.092	0.225	0.060	0.188
ED3	0.038***	0.458***	0.071***	0.505***	0.072***	0.571***	0.132***	0.547***
	(0.011)	(0.074)	(0.024)	(0.084)	(0.015)	(0.081)	(0.034)	(0.095)
Observations	282	282	282	282	282	282	282	282
R^2	0.052	0.227	0.038	0.258	0.101	0.201	0.074	0.190
Adjusted R^2	0.048	0.224	0.034	0.255	0.098	0.198	0.071	0.187
ED4	0.035***	0.452***	0.067***	0.524***	0.070***	0.512***	0.134***	0.518***
	(0.011)	(0.071)	(0.024)	(0.073)	(0.015)	(0.081)	(0.034)	(0.091)
Observations	282	282	282	282	282	282	282	282
R^2	0.045	0.226	0.035	0.286	0.097	0.166	0.077	0.175
Adjusted R^2	0.041	0.223	0.032	0.283	0.094	0.163	0.074	0.172

*p<0.1; **p<0.05; ***p<0.01

Notes: The term premia and risk-neutral yields are estimated using the OSE: ∇y_t model. The regression is $\Delta^{FOMC} y_t^{(n),\cdot} = \beta_0 + \beta_1 HFS_t + \varepsilon_t$. The dependent variable $\Delta^{FOMC} y_t^{(n),\cdot}$ is the daily changes in the n-year term premium or term premium on the FOMC announcement dates or the $t-1$-to-$t+1$ changes around FOMC announcement dates. TP5 and RNY5 denote the 5-year term premium and risk-neutral yields, and those for the 10-year yield are denoted analogously. The high-frequency shock HFS_s is the 30-minute change in the policy rate futures rate bracketing the FOMC announcement time. The shocks are changes in ED1-ED4 during 30-minute windows bracketing FOMC announcements, available on Michael Bauer's webpage for Bauer and Swanson (2022b).